Construction of the Full-Scale Prototype of a BOS MDT Chamber

V. Bartheld, U. Bratzler, D. Kalkbrenner, H. Kroha, Th. Lagouri, A. Manz, A. Ostapchuk, S. Schael

Max-Planck-Institut für Physik,
Föhringer Ring 6, D-80805 Munich

Abstract

The full-scale prototype of a BOS MDT chamber has been constructed at MPI Munich as a common effort of several ATLAS muon institutes following the specifications in the ATLAS Muon Technical Design Report (TDR). The 432 drift tubes in the chamber have been produced at MPI, with support by JINR Dubna and NIKHEF, and fully tested according to the quality control specifications in the TDR at LMU Munich. The spacer frame, including the RASNIK in-plane alignment system, was designed and constructed by NIKHEF. The gas distribution system and the Faraday cages were designed by the University of Freiburg. The HV boards were designed and fabricated by Boston University, the readout boards by BNL. The assembly jigging was set up in a temperature-controlled clean room at MPI where the glueing of the multilayers took place between 26 January and 16 February 1998 including extensive measurements of the mechanical accuracy. The completed chamber has been scanned in the X-ray tomograph at CERN and has taken data in the test beam at CERN.

Contents

1 Introduction

The full-scale prototype of a BOS MDT chamber has been constructed at MPI Munich in a common effort of several ATLAS muon institutes following the specifications in the ATLAS Muon Technical Design Report (TDR) [1]. The goal was to demonstrate that with the barrel chamber assembly method for series production as described in the TDR, the specified accuracy of 20 μm rms in the relative wire positions at the tube ends can be achieved as well as the required tolerance of 100 μm on the centering of the wires within the tubes over their whole length. For the 2160 mm wide BOS chambers, this requires the use of a force compensation system to eliminate gravitational sag of the cross plates. This system, as described in the TDR [1], was first used and demonstrated during the construction of the BOS prototype chamber.

The BOS chambers are among the largest in the barrel with a tube length of 3800 mm and a width of 2160 mm containing 72 tubes per layer and 432 in total in 2×3 tube layers. The layout of the prototype chamber is shown in Fig. 1. At the end for the high-voltage connection to the tubes (HV side), the long beams are connected by a plate to which one of the three bearings for the 3-point support of the chamber is connected. The other two supports are connected to the two long beams at the opposite ends.

All tubes have been produced at MPI Munich with manpower support from JINR Dubna and NIKHEF. They were fully tested at LMU Munich according to the quality control specifications described in the TDR [1]. The spacer frame including the RASNIK in-plane alignment system, as described in the TDR [1], was designed and constructed by NIKHEF. The gas distribution system and the Faraday cages were designed by the University of Freiburg. The HV boards were designed and fabricated by Boston University, the readout boards at BNL.

The assembly jigging for the BOS chamber, as described in detail in the TDR [1], was set up on a granite table in a temperature-controlled clean room at MPI where the glueing of the tube layers took place between 26 January and 16 February 1998 including extensive measurements and verification of the mechanical accuracy. The completed chamber has been measured with the X-ray tomograph at CERN and has been tested in the H8 muon beam at CERN.

2 Tube Production and Test

The 3800 mm long tubes were produced by ALU-MENZIKEN and cleaned in a facility at CERN according to the TDR specifications [1]. In a sample of 100 tubes, the outer diameter at the ends was measured to be (29.975 ± 0.005) mm with a cutoff of the gaussian distribution at 29.970 mm [2].

The tubes have been wired with the MPI glueing method which locates the wires in the tubes in always the same position with respect to the combs holding the tubes which are identical for tube wiring and chamber assembly. Each tube is placed in the combs for wiring and chamber assembly in the same azimuthal orientation around the tube axis in order to minimize sensitivity to tube non-roundness. The wire was positioned relative to the combs holding the tubes simultaneously at both tube ends and fixed in the position with glue curing fast under the illumination with UV-light. The wiring method and setup are described in detail in [3], [4].

The endplug compatible with the wiring method and used for the BOS chamber prototype is shown in Figs. 2 and 3 and described in the TDR[1] and in detail in [3]. The total tube length, including endplugs, was adjusted to ± 0.5 mm during the insertion of the endplugs into the tubes. Uniformity of the tube length is not critical for the parallel gas connection used for the BOS prototype.

The tubes were wired at MPI in a dust-free, temperature-controlled room. The results of the quality control tests at LMU Munich are described in [3]. The wire tension and sag was measured to be equal for all tubes within 1% rms. The wire position at the tube ends was measured for each individual tube with the X-ray method [1]. Results for the wire coordinates y and z are shown in Figs. 4 and 5 separately for the tubes in each of the two multilayers of the BOS chamber and for the two tube ends (sides A and B). Side A corresponds to the HV side of the chamber for multilayer 1 (glued first) and to the readout (RO) side for multilayer 2. The tubes for the first multilayer were produced first.

The standard deviations of gaussian fits to the wire coordinate distributions from the X-ray measurements of individual tubes are $8 - 12$ μm. The tubes were held in the V-blocks for X-ray measurement in the same way as they are placed in the combs used for chamber assembly. Since at the begining of the measurements the absolute calibration of the X-ray device was still uncertain, in Figs. 4 and 5 the wire positions with respect to the tube centers were determined as the average of the wire positions measured in two orientations of the tube around the tube axis relative to the jig, in the same orientation as during tube wiring and after rotation by 180° (see [3]). Therefore in the wire position distributions in Figs. 4 and 5, variations in the tube outer diameter are still folded in.

For the tubes used for the second multilayer, the short-distance straightness near the ends was significantly worse and outside the specifications (see [1]) compared to the tubes for the first multilayer. This affects the reproducibility of the placement of the tubes in the jigs and therefore the wire position for the X-ray measurements and chamber assembly.

In the second multilayer, the average wire position in the y-coordinate on side A of the tubes is shifted by 37.5 μm outwards from the middle plane of the chamber with respect to the nominal position. With respect to the tubes of the d first multilayer, the shift in the average wire position is 25.5 μm. This shift became apparent from the evaluation of the X-ray measurements of the tubes when a major fraction had already been fabricated. It was not corrected for the wiring of the remaining tubes, so it would be common for all tubes in the second multilayer. This was later reproduced in the X-ray tomograph measurements at CERN (see below).

The shift was caused by a vertical tilt of the wiring jigs on side A relative to the jigs on side B which could be traced back to contruction work in the building going on at the time when the displacement occurred. In the provisional wiring setup for the tubes of the prototype chamber, the jigs for both tube ends were installed on separate tables; a movement of the floor under one table could cause a tilt as it was observed. In the final wiring setup, the jigs for both tube ends will be mounted on a common table and their relative orientation as well as the wire position with respect to the tube jigs will be continuously monitored, so that such displacements will be prevented.

3 Assembly Setup

The chamber assembly jig used for the construction of the BOS prototype has been described in detail in the TDR [1]. The setup installed on a granite table of size 4200 mm × 2500 mm is shown in Fig. 6. The assembly table is set up in a temperature-controlled clean room of class 100000. The working temperature of 20° was stabilized to ±0.5° within the volume of 2 m height above the surface of the table. A temperature difference of 0.1° has been measured between the top and the bottom of the chamber on the assembly table. Humidity was controlled to be (45 ± 5) %. Clean room clothes and gloves were used during the installation of the jigging and the whole assembly procedure.

The tube jig is assembled out of comb modules with 20 tube positions each. 9 comb lines are installed on the granite table at a distance of 500 mm (300 mm for the two comb lines at the tube ends). Each comb line consists of 4 comb modules. The layout is shown in Fig. 7. Each tube layer of the BOS chamber consists of 72 tubes. The comb lines were aligned in the z coordinate with respect to the precise edge of the granite table (the reference side; see below) and in x with a 2 m long granite ruler. The comb lines can expand or shrink with temperature variations along the z direction from their fixation point at the reference edge of the granite table.

The precision comb modules (see Fig. 8) were produced completely industrially. They are cut out of hardened FORTAL 7075 aluminum plates using electric spark erosion. The comb modules were produced in triplets in the wire erosion process. The V-groove design of the comb modules is shown in Fig. 9. It minimizes sensitivity of the tube vertical (y) positions to tube outer diameter variations. Fig. 8 illustrates the installation of the comb modules on the granite table. More details are given in the Appendix.

All comb modules have been measured on a 3D measuring machine by placing precise steal cylinders of 30.000 mm diameter in the V-grooves. Results for the z-pitch and the vertical (y) position of the cylinders are shown in the TDR [1]. The average horizontal (z) pitch of the 36 comb modules was measured to be (30.0366 ± 0.0008) mm. The measured horizontal (z) spacing and the height (y) of the V-grooves of individual comb modules showed rms errors of $1-9$ μm (majority $2-5$ μm) and $1-8$ μm (majority $2-5$ μm), respectively.

The 8 best comb modules with respect to uniform height (y coordinate) were selected for the comb lines at the tube ends. Distributions of the z-distances and of the residuals from the nominal value of the y-position of test cylinders inserted in the V-grooves are shown in Figs. 10–13 for the tube positions 1–72 of the two end comb lines. The rms values of the height distributions are $3-4$ μm. The z-pitch of the end comb lines is 30.0368 mm with a dispersion of the z-distances of the V-grooves of 5 μm. Some of the end comb modules show significantly larger scattering of the z-distances than the others (see Figs. 10 and 11). Here is room for improvement by better selection of end comb modules which was not done for the prototype chamber because of lack of time.

4 BOS Chamber Assembly

4.1 Insertion of Tubes

During the assembly, the tubes are held down in the V-grooves using vacuum suction pads with 15 mm diameter in the end combs (suction force of about 400 g) and with 8 mm diameter in the intermediate combs. The tubes are held in the end combs 25 mm from the

Table 1: Vertical layer spacing $\Delta y - \Delta y_{\rm nominal}$ [μm] ($\Delta y_{\rm nominal} = 26.011$ mm): comparison of installed sphere block height, mechanical measurements from the combs to the tube walls glued on the spacer and X-ray tomograph measurements of the wire positions. The measurement accuracy in all cases is $5 - 10$ μm.

$\Delta y - \Delta y_{\rm nominal}$ [μm]	Tower height		Tube walls		X-ray scan	
Layers	RO side	HV side	RO side	HV side	RO side	HV side
1–2	+35	+35	+34	+40	+47	+51
2–3	+50	+50	+34	+41	+48	+48
4–5	+30	+30	+24	+24	+38	+42
5–6	+55	+55	+36	+40	+62	+44

tube ends. Measurements of the relative y-position of wired tubes (height of the top of the tube above the granite table measured with a feeler gauge) in the end combs on the HV and the readout side (tube sides A and B, respectively, during glueing of the first multilayer) are shown in Fig. 14. The widths of the residual distributions are $7 - 8$ μm which include the effect of tube outer diameter variations and uncertainties in the correct placement of the tubes in the V-grooves.

The horizontal glue gap between the tubes inserted in the combs was verified by visual inspection along the whole tube length with illumination of the tube layer from below. This method was found to be the most efficient one for the detection of touching tubes due to tube non-straightness or problems with the suction of the tubes into the combs. Situations where several adjacent tube get displaced are critical with respect to the wire concentricity requirement. They could all be detected and resolved in this way by relocating tubes; no tubes had to be rejected because of non-straightness in between the combs.

4.2 Vertical Stacking of Tube Layers

For the vertical stacking of the tube layers, the spheres mounted at both sides of the cross plates are supported on 6 sphere blocks (towers; see [1]) which are increased in height for successive tube layers within a multilayer using precisely machined distance plates. Compressibility in the tower height of approximately 10 μm under the load of the chamber was found during the first tests of the assembly setup and confirmed by dedicated measurements. The origin was identified to be the ball bearings on which the spheres are supported moveable in the $x-z$-plane and which make imprints in the base plates. The compressibility may be reduced to a certain degree by more thorough hardening of the base plates.

Exceptions with respect to the degrees-of-freedom of the sphere supports are two towers at the chamber ends on one side of the assembly table (defined therefore as the reference side): one is fixed in both coordinates and the second one constrained to movements in x-direction to ensure relative alignment of the tube layers with respect to rotations around the y axis. The middle tower on the reference side must allow for free movements of the sphere in x and z. Otherwise the support of the chamber on the spheres is over-constrained, especially after stiffening by one or more tube layers glued, which leads to incorrect and irreproducible y positions of the spheres on the towers.

Because of concerns about the height stability of the sphere blocks under load after initial

tests, the uncertainties in the cross plates sag compensation and the associated cross plate movements in y and because of observed enlarged tube outer diameters near the tube crimp location, it was decided to increase the vertical wire spacing by 30 μm from the nominal value of $\Delta y_{\rm nominal} = 26.011$ mm (corresponding to a layer-to-layer wire pitch of 30.035 mm) in order to avoid touching of tube layers at any instance during assembly. The extra vertical spacing was created by adding steal foils to the tower height and verified by measuring with gauge blocks the distance from the combs to the outer walls of the tube layer(s) already glued to the spacer (see Table 1). The resulting increased vertical wire pitch of on average 26.054 mm from increased tower heights was reproduced in the X-ray tomograph measurements with an average y-pitch of 26.059 mm (see Table 1).

4.3 Force Compensation for the Cross Plates

The sag of the cross plates under the weight of the spacer and of the glued tubes layers was eliminated by a force compensation system with 4 removable bars inserted through the long beams at the inside of the two outer cross plates and on both sides of the middle cross plate (see the TDR [1] and Fig. 6). The force compensation bars are supported at both ends on the granite table with with screws to adjust the height and therefore the force. For series production, automatic pneumatic adjustment and measurement of the forces applied to the force compensation bars is desireable. For the prototype construction, independent manual adjustment of all force compensation bars was useful to study the principle and its limitations (see Table 2).

The sag of the cross plates was measured with RASNIK systems installed on the side of each cross plate over its full length. The RASNIK in-plane alignment system and the RASNIK systems on the cross plates were calibrated by placing the spacer on the jigging (sphere towers) and reading the RASNIK measurements in an initial (INI) position and in the inverted (INV) position after rotation around the x axis by 180° (see Figs. 15 and 16). The cross plate sag is the average of the on-cross-plate RASNIK readings in initial and inverted position if the forces of the long beams on the cross plates are symmetric for both orientations, i.e. if there are no stresses built into the chamber. The calibration measurements were repeated after glueing of each tube layer and monitored carefully. The zero-positions of the in-plane RASNIK lenses were stable within ± 5 μm in z and ± 10 μm in y over the whole assembly procedure. The y calibration readings are affected by incomplete compensation of the middle cross plate sag (see below). The optical monitoring systems were read out and watched continuously during the whole assembly operation.

The gravitational sag of the middle cross plate could be measured with the on-cross-plate RASNIK system only during glueing of the first multilayer. For the assembly of the second multilayer the on-cross-plate RASNIK monitor on the middle cross plate had to be removed for space reasons since the design of the BOS chamber spacer had not forseen the installation of on-cross-plate sag monitors. However, from the combined data of the in-plane alignment system and the RASNIK systems on the outer cross plates, the sag of the middle cross plate can be reconstructed with high accuracy. This was verified during all operations of the assembly of the first multilayer by comparing the direct and the indirect measurements of the middle cross plate sag (see Fig. 17). In the future, an on-cross-plate RASNIK system on the middle cross plate can therefore be avoided.

The long beams were adjusted to the center of the middle cross plate with an accuracy of ± 50 μm by comparing the spacer sag measurements of the longitudinal RASNIK in-plane

Table 2: Sag of the high-voltage (HV), readout (RO) and middle (MI) cross plates supported on the sphere towers before and after force compensation with increasing number of tube layers glued (with y-axis pointing upwards). The number of turns of the force adjustment screws needed to reach compensation are given in the last column. (Note that after glueing of layer 4 a readjustment of the fixations of the force compensation bars to the long beams was done and that therefore the number of turns needed cannot be compared with previous ones.)

Layers	Cross plate	Initial sag	Compensated	# Turns
0	HV	-28 μm	$-$ 2 μm	5
	MI	-36 μm	$-$ 7 μm	3
	RO	-29 μm	$-$ 5 μm	5
1	HV	-28 μm	0 μm	6
	MI	-37 μm	+ 1 μm	3.5
	RO	-27 μm	+ 1 μm	6
2	HV	-28 μm	$-$ 1 μm	6.5
	MI	-39 μm	+ 2 μm	4
	RO	-29 μm	$-$ 2 μm	6.5
3	HV	-38 μm	$-$ 3 μm	8
	MI	-52 μm	-16 μm	4.5
	RO	-39 μm	-11 μm	8
4	HV	-47 μm	$-$ 6 μm	5
	MI	-59 μm	-17 μm	3
	RO	-42 μm	$-$ 8 μm	5
5	HV	-39 μm	$-$ 5 μm	5
	MI	-63 μm	-16 μm	3
	RO	-40 μm	-10 μm	5

alignment systems on both sides of the chamber while the spacer was held in vertical position on the crane at the support points on the plates connecting the long beam ends. After this adjustment, the readings of the on-cross-plate RASNIK systems in the two vertical positions of the spacer on the crane (V1, V2) are in the middle between the readings in the initial and inverted position of the spacer on the table as expected for vanishing cross plate sag (see Figs. 15 and 16). The cross plates sags in the initial (INI) and inverted (INV) position are now symmetric (same absolute values with opposite signs) with respect to the vertical calibration measurements and can now be used as references for the force compensation adjustment.

In the two horizontal (H1, H2) positions of the spacer on the crane, the cross plates are slightly curved upwards (see Figs. 15 and 16) due to the additional weight of the spheres which holds them on the sphere support towers even with full force compensation.

After the long beam adjustment and the RASNIK calibration, the RASNIK measurements on the cross plates can be used to adjust the force compensation: The screws of the force compensation bars were turned sequentially in steps until the measured curvature of all three cross plates was minimized. The RASNIK sag measurements before and after force compensation with increasing number of tube layers glued are given in Table 2 and Fig. 18. The rather large cross plate sag of the 2160 mm wide BOS chamber makes force

Table 3: Sag (along the x-direction) of the chamber supported on the crane in the two horizontal positions (initial and inversed) with increasing number of tube layers during assembly. The sags measured with the longitudinal RASNIK monitors along the two sides of the chamber as well as the average sag are shown. The last row corresponds to the completed chamber without the weight of the spheres attached to the cross plates during assembly.

	Initial			Inversed		
Tube layers	Side 1	Side 2	Average	Side 1	Side 2	Average
0	444	366	404	447	367	407
1	430	356	393			
2	471	394	432			
3	485	416	450	484	434	454
4				471	429	450
5				502	453	481
6	504	470	487	522	490	506
6	423	381	402	424	402	413

compensation necessary to achieve the required precision in the wire positions and to avoid touching of tube layers during the stacking process. For the latter, the force compensation must act instantaneously when the spacer frame is lowered on the sphere blocks. Therefore the force compensation was adjusted in advance as described above before the next layer of tubes was inserted in the combs and the spacer frame was lowered again. The heavy bearings for holding the chamber on the crane caused additional cross plate sag of 5 μm and were removed during force compensation and glueing and for the measurements in Table 2 and Fig. 18.

After force compensation, the residual sag of the outer cross plates was below 5 μm for the first multilayer glued (the goal) and at most 10 μm for the second multilayer which is sufficient for the required chamber accuracy. For the middle cross plate which carries a larger load than the outer cross plates, the remaining sag was ≤ 7 μm for the first multilayer and ≤ 17 μm for the second multilayer. Between the tube ends the tube positioning requirements can be relaxed; the wire position is not affected by the tube position and the tolerance on the concentricity of wire and tube is only 100 μm. No additional weights were used to hold the spheres in position in their supports during force compensation. Additional weights will help to achieve complete compensation up to the maximum number of layers before the spheres are lifted from their supports.

Stacking of the tube layers and the lifting of the spacer during force compensation was monitored with two lasers passing through transparent MPA-ALMY position sensors mounted on the spacers at the sphere holders between spheres and cross plate and on both chamber ends on the granite table as reference (see [1], [5] and Fig. 6). A lifting of the cross plates at the location of the mounted sensors by $20 - 30$ μm was measured with this system (see Fig. 19). It is consistent with the straightening of the cross plates, including the sphere holders mounted on them, between the sphere supports during the force compensation.

The gravitational sag of the chamber along the x-direction with increasing number of glued tube layers was measured with the in-plane alignment system while the chamber was supported almost kinematically on the crane in the two horizontal positions (see Table 3

and Fig. 20). The sag values correspond to the weight of the chamber including the spheres mounted on the cross plate and the steal plates connecting the long beams. For the last row in Table 3, the spheres were removed after completion of the chamber. The sag values were measured with the two RASNIK monitors oriented parallel to the two long beams.

The sag values measured in the initial and the inverted horizontal position agree quite well. The sag values on both sides are different due to internal stresses in the spacer left over after the long beam adjustment on the middle cross plate with an accuracy of ± 50 μm sufficient to make the cross plate sag symmetric in the initial and inversed horizontal position (see above). The difference becomes smaller with increasing number of tube layers adding stiffness to the chamber. The chamber sag adjustment needed in order to match the wire sag is therefore different on the two long beams The measured sags to be compensated deviate from the calculated average sag of a chamber without internal stresses.

4.4 Glueing of the Tube Layers

The tube layers were glued sequentially first for one multilayer and then after turning of the spacer for the second multilayer. The tube layers are numbered in the sequence of glueing. The location of each drift tube in the chamber was recorded. The tubes are identified by numbers engraved before the wiring procedure.

A semi-automatic glue dispenser with two glueing heads moving parallel to the tubes (see Figs. 21, 22 and 28) was used to deposit well defined glue ropes in between and on the tubes inserted in the combs. Araldite 2011 (two-component epoxy) from Ciba-Geigy was used for glueing the tubes to each other. The glue deposition can be shut off automatically and instantaneously at any position along the tubes. 45 minutes were needed for a full layer of 72 tubes of 3.8 m length which is just enough for a setting time of the glue of about one hour. The glue distribution time can be shortened by using premixed glue and/or an additional glue dispenser head.

The diameters of the three glue outlets of each dispenser and the distribution speed were optimised such that the diameter of the glue ropes is not larger than 0.5 mm. The amount of glue on the tubes was minimised to reduce out-of-plane deflections of the tubes between the cross plates when two tube layers are glued together (see the illustration in Fig. 23). The tube deflections have to be controlled in order to keep the 100 μm tolerance on the centering of the wires in the tubes. The effect is expected to be most pronounced for the glueing of the second to the first tube layer in each multilayer since the force of the first-layer to compress the glue is only $1-2$ g/cm per tube.

Out-of-plane deflections of the tubes have been measured in a glueing test where a second tube layer was put on the first one in the combs with a 50 μm spacer foil in between and with weights on top of the tubes layers at the x-positions of the cross plates. Fig. 24 shows the deviations in the tube height from the nominal value for the first layer in the combs and for the second layer glued on top. The measurements were done with a feeler gauge on top of several tubes at the ends of the comb lines where they are accessible. A maximum deviation of 130 μm was observed at the position of the third comb, 80 cm from the tube ends. During chamber assembly, the top tube layer will apply more force on the glue than in this test because these tubes are glued with fixed angle to the cross plates.

To eliminate possible out-of-plane deflections during the assembly of the chamber, weights were put on top of the tube layers already glued to the spacer above the positions of the third and seventh comb, 80 cm from the tube ends, while a 50 μm thick and 1 cm wide

Table 4: Global relative z-shifts between adjacent tube layers and between the two multilayers (ML) as determined from the X-ray scans (the positive z-axis points away from the reference side of the assembly jigging).

Δz [μm]		
Layers	RO side	HV side
1–2	−14	− 2
2–3	− 3	−26
4–5	− 5	− 7
5–6	−23	−12
ML 1–ML 2	−17	−11

aluminum foil was placed at the same positions between the tube layers glued together (see the illustration in Fig. 23). A gap was left for the foils in the glue ropes along the tubes by automatically shutting off the glue dispenser.

Measurements of the tube heights after glueing of the second to the first layer in multilayer 1 (see Fig. 25) and after glueing of the fifth to the fourth layer in multilayer 2 (see Fig. 26). The glued layers are numbered sequentially. The remaining tube deflections are on an acceptible level. Since 50 μm foil is thinner by $30 - 40$ μm than the average vertical glue gap size (compare Table 1), the tubes layers could be pushed together closer at the position of the weights. No significant difference can be observed between the measurements on both sides of the chamber: tubes 1–6 where the glue was distributed first and tubes 67-72 which were glued last. One concludes with a foil of thickness equal to the average vertical glue gap size out-of-plane deflections due to the glue can be virtually eliminated.

The tube layers were glued to the cross plates with Araldite 2014 (two-component epoxy) from Ciba Geigy distributed on top of each tube with a manual glue dispenser with mixer. The shrinkage of the glue, which can lift the tubes from the combs against the suction force of about 400 g, has been measured in the realistic geometry to be below 1% of the glue gap size. Therefore differential glue shrinkage for the existing glue gap variations of $0.2 - 0.8$ mm has negligible effect on the relative positions of the tubes and, therefore, of the wires.

Pictures of the chamber during construction and after completion installed in the test beam area at CERN are shown in Figs. 27–30.

5 Results of X-ray Tomograph Measurements

The completed BOS chamber has been scanned in the X-ray tomograph at CERN [6]. Several scans have been performed along the three cross plates, 9 on the HV side, three on the RO side, three in the middle, for all orientations of the chamber on the 3-point support in the tomograph. All scans are in good agreement with each other within the quoted X-ray tomograph accuracy of about 5 μm.

The horizontal (z) wire pitch was measured to be 30.0360 mm which coincides exactly with the comb pitch. Table 4 shows the measured relative shifts between tube layers and between the multilayers in z-direction with respect to the nominal positions. The measured average vertical (y) wire pitch of 26.059 mm is in agreement with the expectation (compare

Table 1).

The measured average y-distance between the two wire planes closest to the spacer in both multilayers (layers 1 and 4) from all X-ray scans is $\Delta y_{\rm meas}^{\rm spacer} = 347.040$ mm on the HV side and 347.078 mm on the RO side with an uncertainty of about ± 10 μm. The measured values agree exactly with the expectations from the chamber assembly tooling. The measured sphere block height of 276.550 mm and the height of 118.030 mm of a 30.000 mm diameter cylinder on the combs above the surface of the granite table (see Fig. A2) determine the nominal spacer height to be 317.040 mm. The tube wiring method [3], [4] placed the wires with respect to the combs in a position corresponding to the center of a 30.000 mm diameter cylinder inserted in the combs. The expected distance between wire planes of layer 1 and 4 is therefore $\Delta y_{\rm expect}^{\rm spacer} = 347.040$ mm. On the RO side, the relative shift in the average y positions of the wires in the tubes for the first multilayer (side B) and for the second multilayer (side A) increases the expected multilayer distance to 347.072 mm (see Figs. 4 and 5) which is quantitatively reproduced in the

The residuals of the X-ray tomograph measurements of the z and y positions of the wires in both multilayers with respect to the ideal wire grid for the whole chamber (with the expectations for z- and y-pitch and the multilayer distances on HV and RO side) are shown in Figs. 31–33 for scans along the three cross plates. No parameters have been left free to adjust. The data were corrected for the sag of the outer cross plates as measured with the on-cross plate RASNIK systems during the X-ray scans and also seen in the X-ray scan data. The standard deviations of the residual distributions are below the required 20 μm in y and z at both chamber ends (HV and RO side): $\sigma_y(HV) = 17.4$ μm, $\sigma_z(HV) = 17.7$ μm and $\sigma_y(RO) = 16.3$ μm, $\sigma_z(RO) = 14.6$ μm. In the middle of the chamber, the wire positions scatter even less, by about a factor of $1/\sqrt{2}$, as expected from the average of the wire positions at the chamber ends: $\sigma_y(MI) = 12.5$ μm and $\sigma_z(MI) = 13.9$ μm.

6 Conclusions

With the construction of the BOS prototype chamber it has been demonstrated that with the assembly method described in the Technical Design Report for the barrel chambers the required wire positioning accuracy can safely be achieved. It has been shown that the cross plate sag compensation scheme works and that out-of-plane deflections of the tubes between the cross plates can be controlled in a straight-forward way.

Pictures and two short videos of the BOS tube wiring and test and of the BOS chamber assembly are available on the MPI Muon Web Page at http://pcatlas4.mppmu.mpg.de.

References

[1] *ATLAS Muon Spectrometer Technical Design Report*, A. Airapetian et al., CERN/LHCC/97-22, May 1997.

[2] T.Ferbel and A. Manz, *More on Dimensions of Menziken Tubes*, ATLAS Internal Note, MUON-NO-209, August 1997.

[3] U. Bratzler et al., *Assembly and Test of the Drift Tubes for the BOS MDT Prototype Chamber*, ATLAS Internal Note, MUON-NO-xxx, October 1998.

[4] U. Bratzler al., *The MPI Endplug and Tube Wiring Technique*, ATLAS Internal Note, MUON-NO-xxx, October 1998.

[5] H. Kroha and S. Schael, *Optical Monitoring System for the MDT Assembly Stations*, ATLAS Internal Note, MUON-NO-156, April 1997.

[6] D. Drakoulakos et al., *The High-Precision X-ray Tomograph for Quality Control of the ATLAS MDT Muon Spectrometer*, CERN-OPEN-97-023, July 1997.

7 Appendix: Design and Fabrication of the Assembly Jigs

7.1 Parameters and Fabrication of the Comb Modules

The wire erosion technique for the fabrication of precision combs uses a bath with 680 mm maximal length. The combs of the tube jig are assembled out of shorter modules. The width of the BOS chambers of 2160 mm is the largest chamber width with 72 tube per layer. The comb lines in this case are assembled with the maximum number of 4 modules for 20 tubes each.

The wire erosion process proceeds in several computer controlled cutting steps. The process has been optimized in collaboration with the company. A set of precise pin holes of 10 mm diameter is eroded in the first cutting step. The holes allow to reproduce the position of the piece in the erosion machine. Typically five cuts are used to reach the specified precision (see below). Before the last cut the module is measured on a certified machine. Systematic deviations of the pitch as function of the tube position are compensated for in the last cut.
The following parameters of a comb module (see Fig. A1 and A2) have been chosen:

- The shape of the V-groove is formed by two circles of 16 mm radius with shifted centers.
- The opening angle of the V-groove is optimised to be 90 degrees. The optimisation includes minimum deformation of the tubes and minimum effect of tube diameter variations and of comb errors.
- The pitch of the comb modules was defined to be 30.035 mm. Systematic deviations in the fabrication process are specified to be less than 5 μm over the module length, with rms errors less than 2 μm.
- The comb module width of 25 mm is determined from considerations of minimum deformations of the tubes under typical forces vs. cost aspects.
- The height of a comb module is 94 mm. Two support feet make contact to the granite table. The sag of individual modules is negligible. The height gives sufficient space e.g. for vacuum lines.
- The vacuum suction cups are flexible silicon rubber pads (NIKHEF type) which will be imbedded directly into the V-grooves (see Fig. A3).

7.2 Assembly of the Tube Jig

Each comb module has reference surfaces for the assembly and adjustment in the z direction. Two precision calibers define the distance between modules and keep the pitch correct (see Fig. A3). Even with the slight overconstraint, the module position will be kept within tolerances. A screw in the neutral line holds two adjacent modules together. Shimming is possible but probably not necessary.

The granite table used for chamber assembly at MPI has a second precisely polished surface on one side (the reference side). The side and top surfaces of the table form a precise reference system. The combs assembled out of 4 comb modules are aligned with respect to

the side surface. A comb is fixed relative to the side surface in only one point allowing for thermal expansion of the comb. Alternatively, an additional precise granite bar can be used to replace the precise side surface.

On the granite table there is a pattern of threaded holes. They are used to install for each comb an aluminum fixation bar (see Figs. A4 and A5). A second bar connected to the first one is used to press down the comb with an adjustable force. A set of screws allows to adjust each comb module perpendicular to the side surface (Fig. A7). The fixations in x and y are such that the long comb line can thermally expand without stresses in the z direction. All the tooling is arranged on one side of the comb line, the other side is accessible for measurment of positions and angles.

The vacuum is distributed independently for each comb module (see Fig. A6) such that the vacuum can be switched selectively for subsets of tubes and along the tubes.

Hardened aluminum (7075 FORTAL STS with hardness of 140 Brinell) was chosen for the fabrication of the combs. It was thermally treated to take out stresses.

To test abrasion of the combs by inserting tubes, a tube was put 1000 times into a V-groove of a comb module made of less hard aluminum from a previous comb production which had a width of 12 mm. The tube was turned each time by 90 degrees under a load of 380 g. The change in the vertical y position due to possible material abrasion was measured after every tenth trial. Fig. A8 shows the change in the y position of the tube over 1000 trials (100 measurements). The maximum abrasion over the whole chamber production is only 10 μm which is well acceptable. Differential abrasion in the different V-grooves which could affect the chamber precision will be negligibly small.

Acknowledgements

The authors thank the members of the Technical Division of the Max-Planck-Institute for their enormous effort during the preparation of the chamber assembly setup, the fabrication of the drift tubes and the final construction of the chamber. We also thank our collegues from Ludwig-Maximilian University, Munich for the careful and patient testing of the drift tubes.

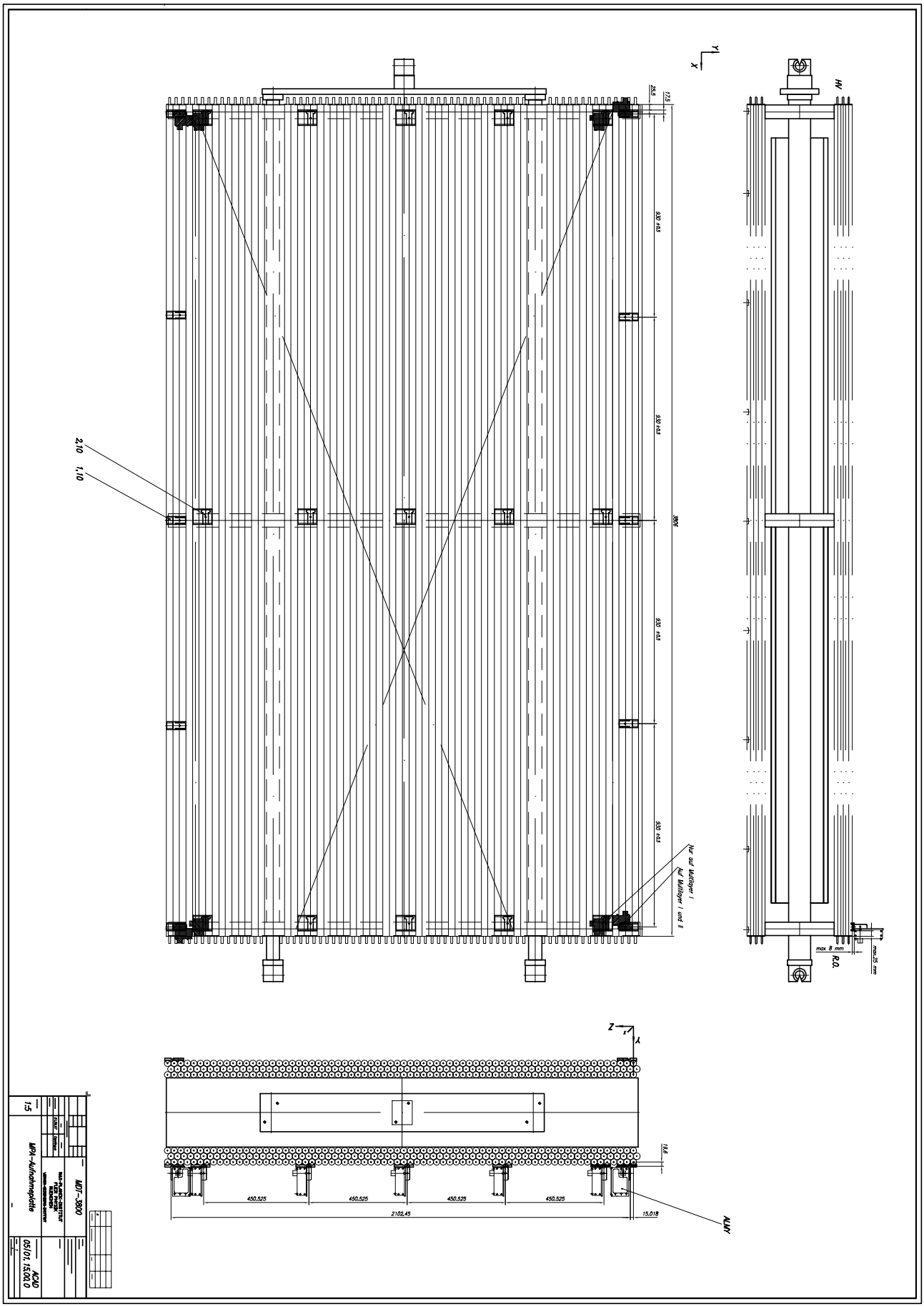

Figure 1: Dimensions of the BOS prototype chamber. The locations of mounting plates for alignment sensors (MPA-ALMY sensors) are indicated.

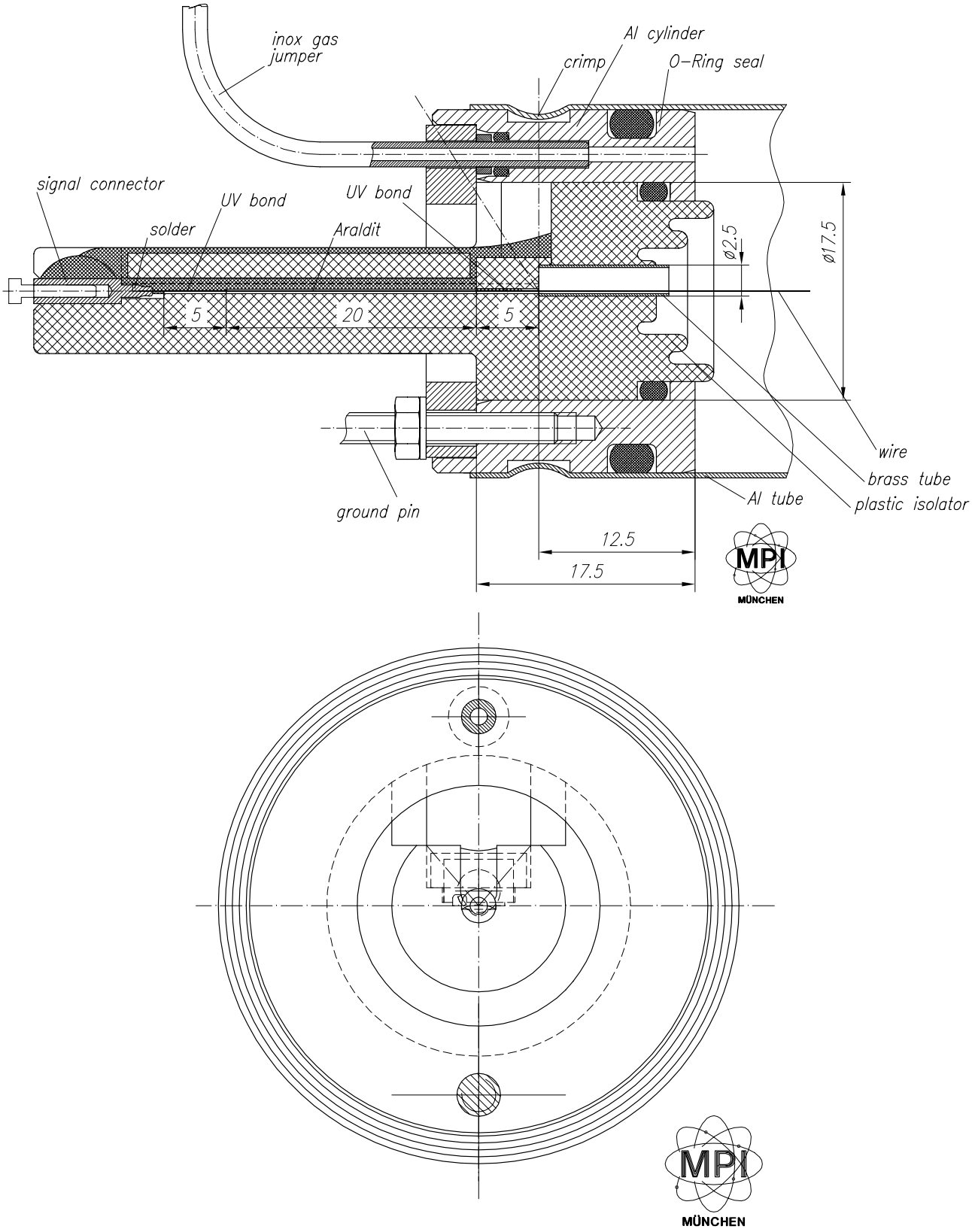

Figure 2: Drawings of the endplug for the tubes of the BOS prototype chamber: longitudinal cross section and front view.

Figure 3: Endplug and drift tubes for the BOS prototype chamber.

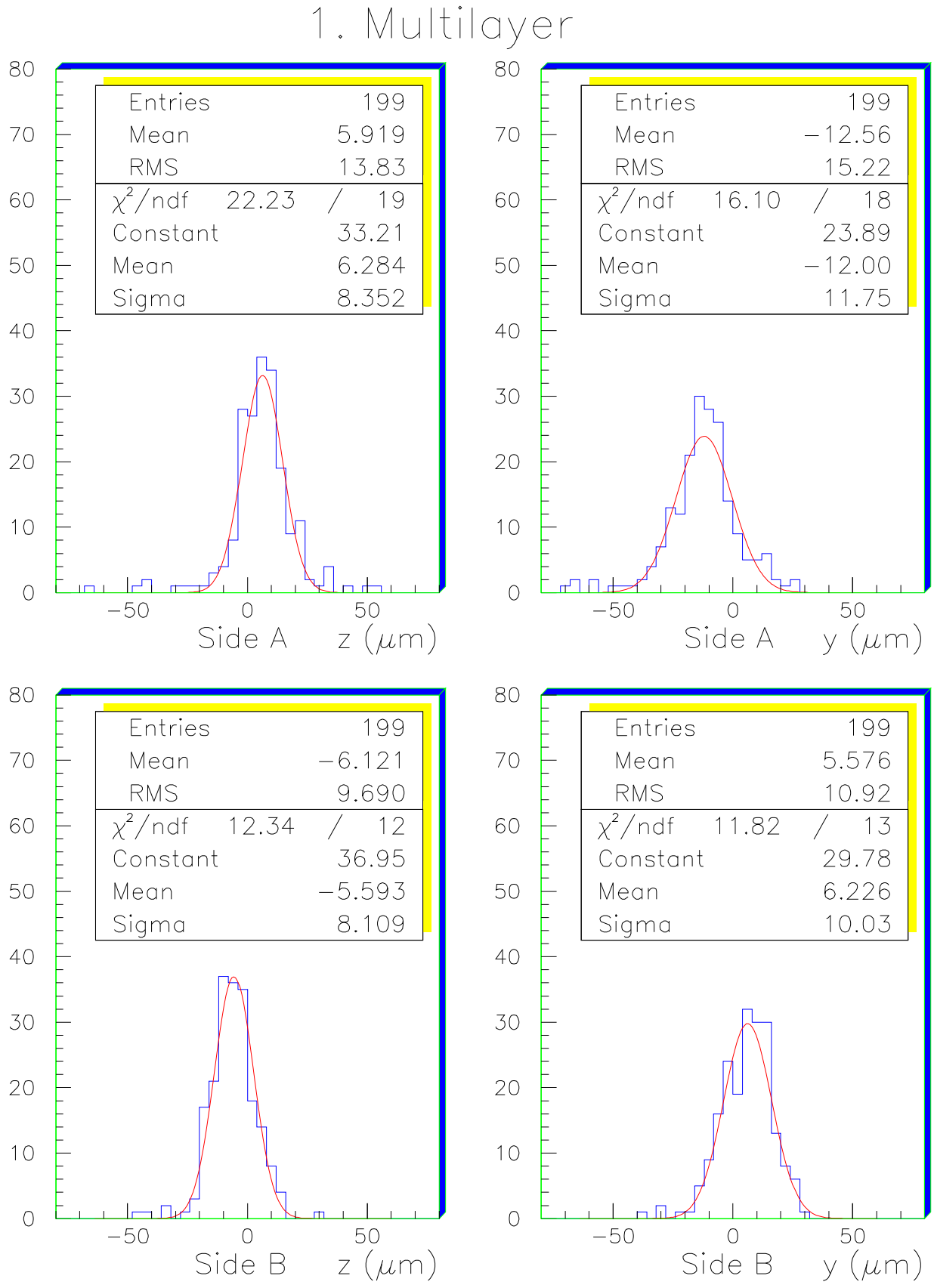

Figure 4: Wire coordinates y and z measured with the X-ray method for side A and B of the tubes in the first multilayer.

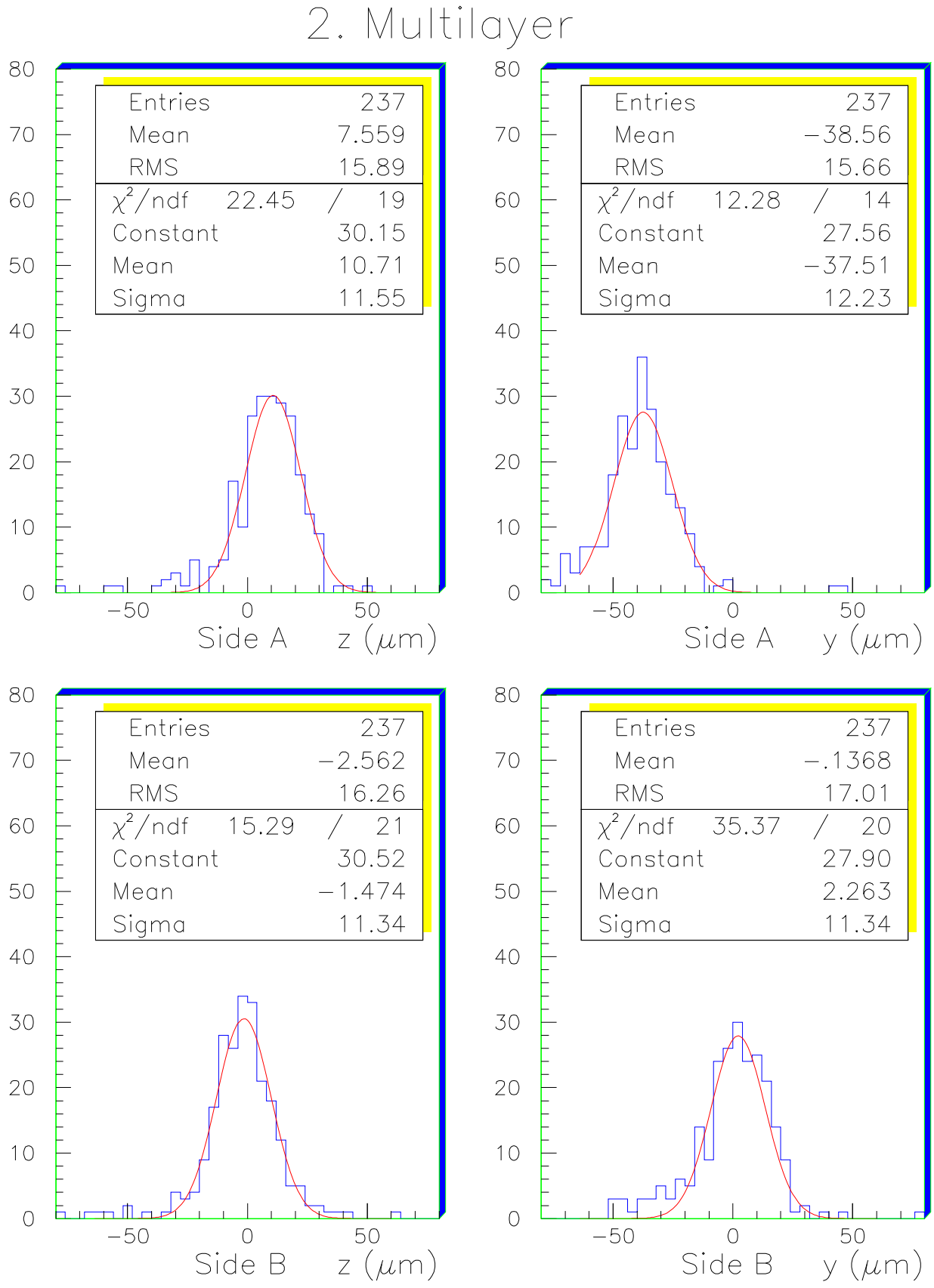

Figure 5: Wire coordinates y and z measured with the X-ray method for side A and B of the tubes in the second multilayer.

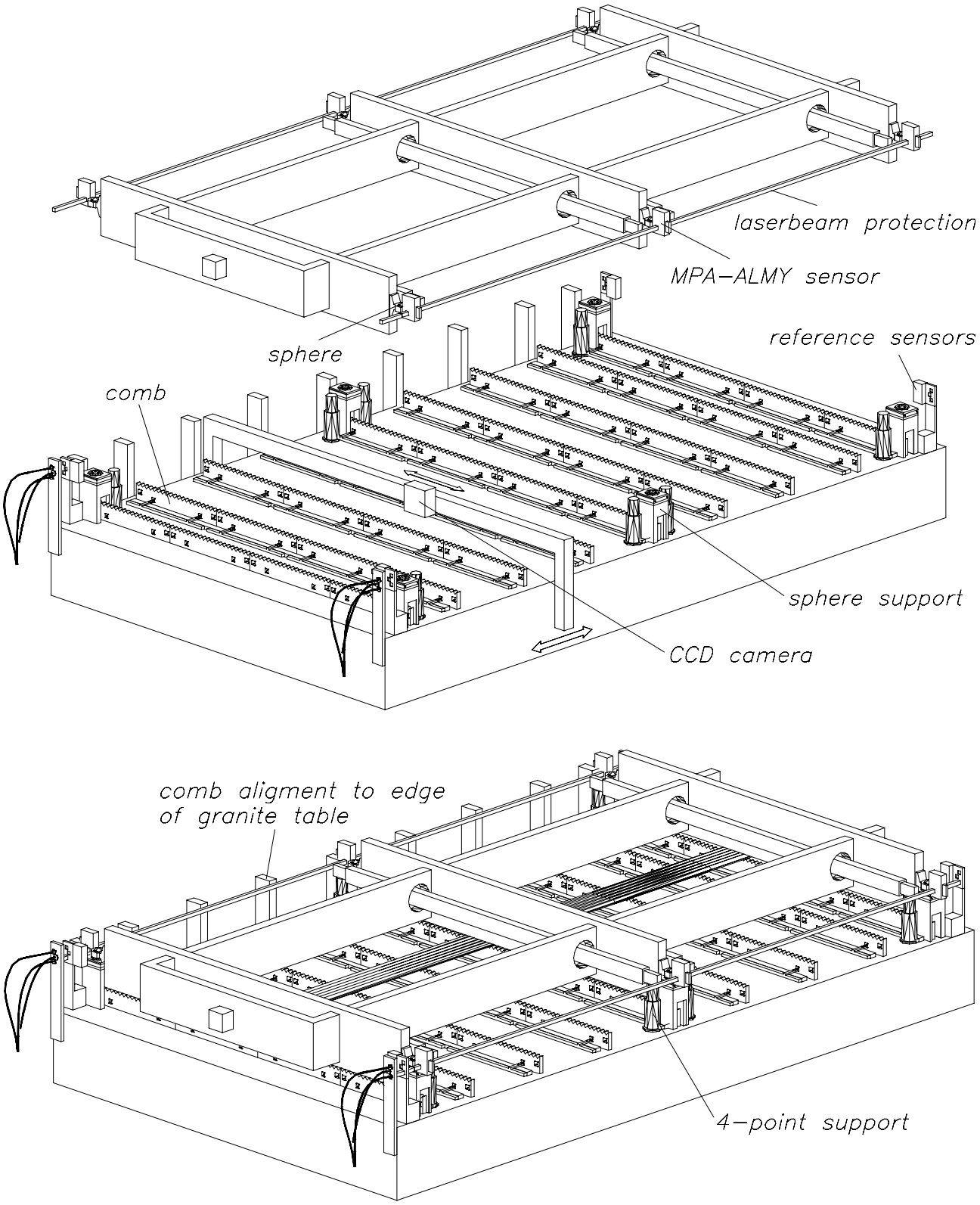

Figure 6: Assembly jig setup with monitoring devices for the BOS chamber construction.

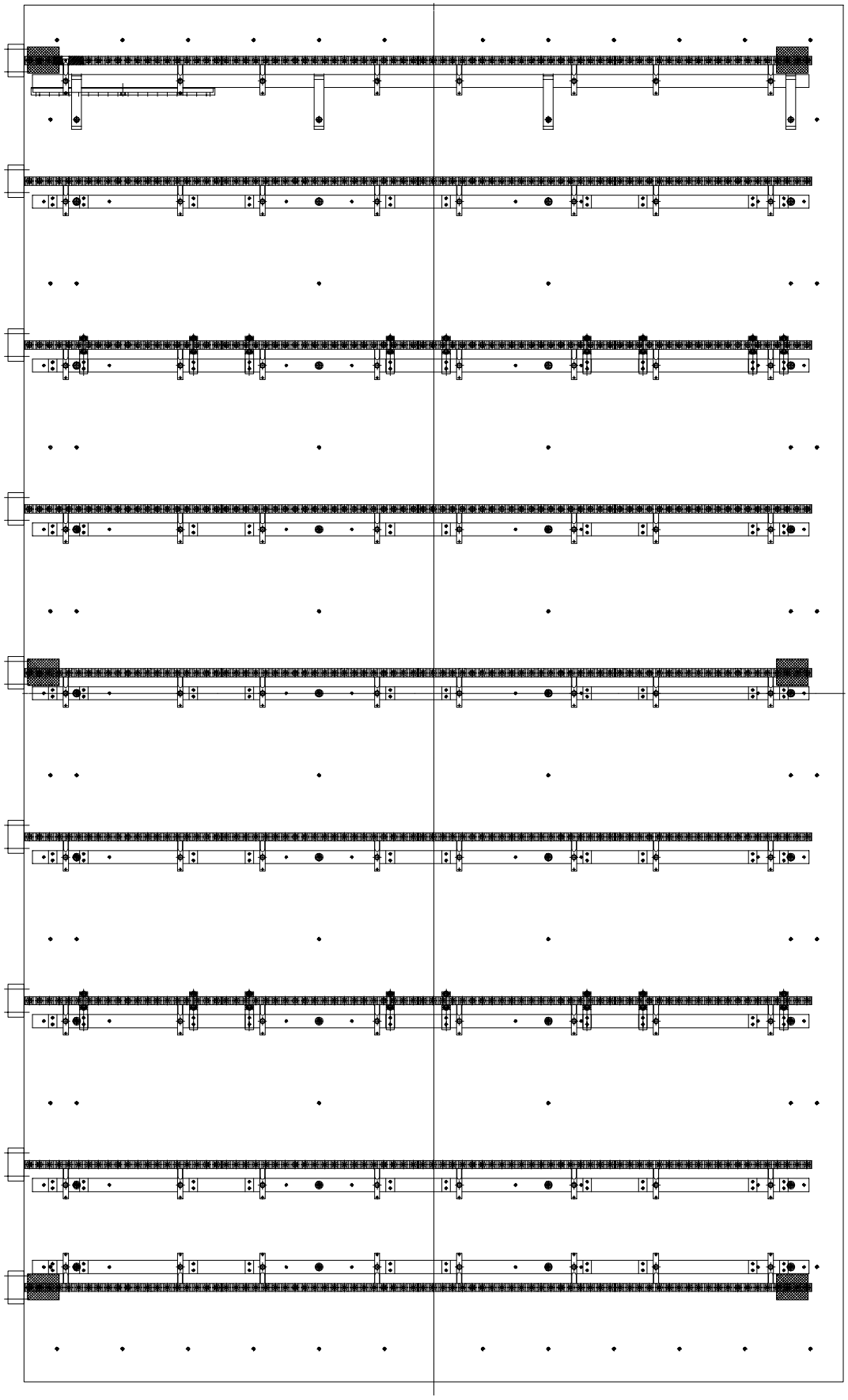

Figure 7: Layout of the comb lines on the granite table.

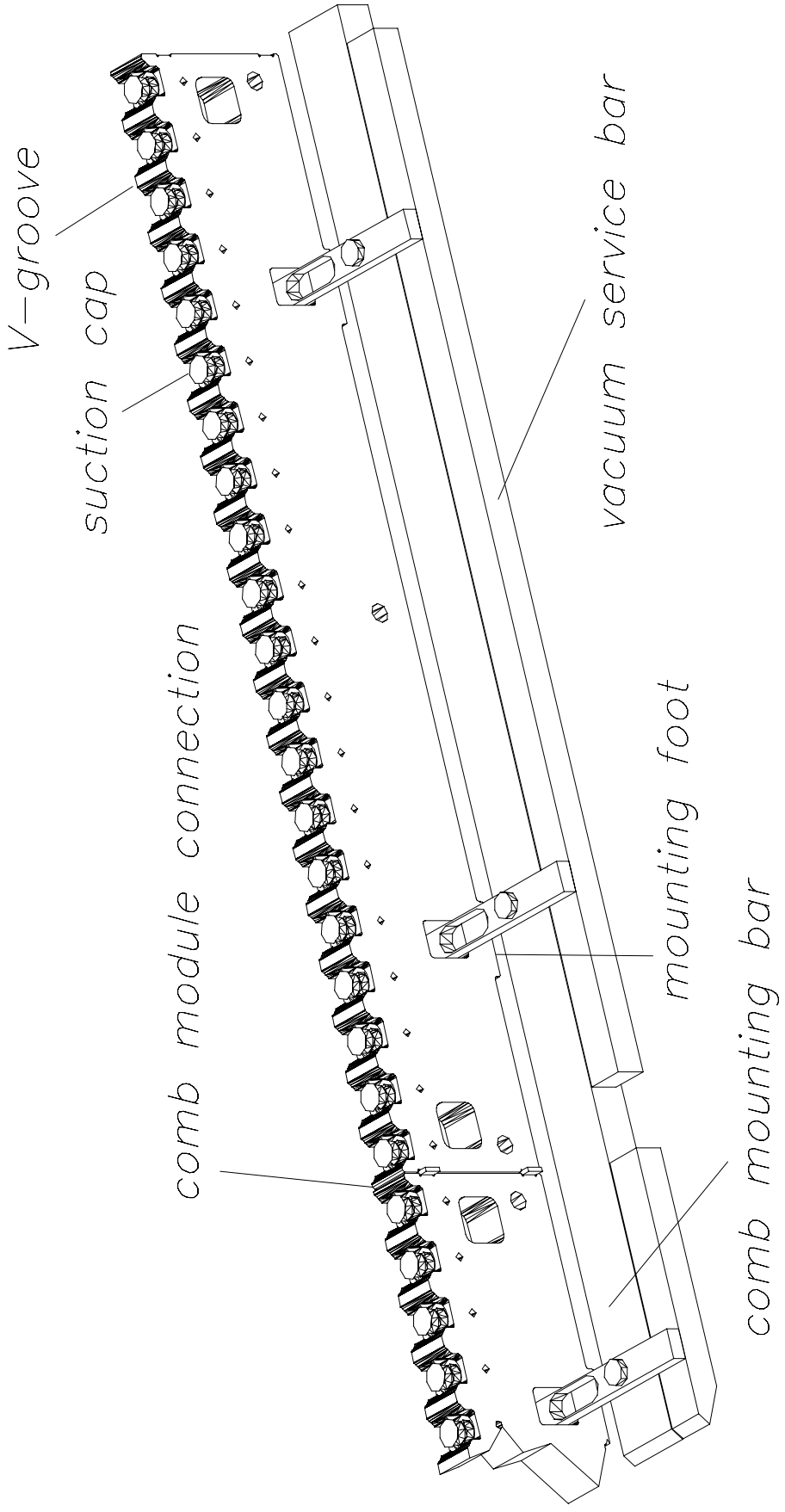

Figure 8: 3D picture of a comb module for the tube jig.

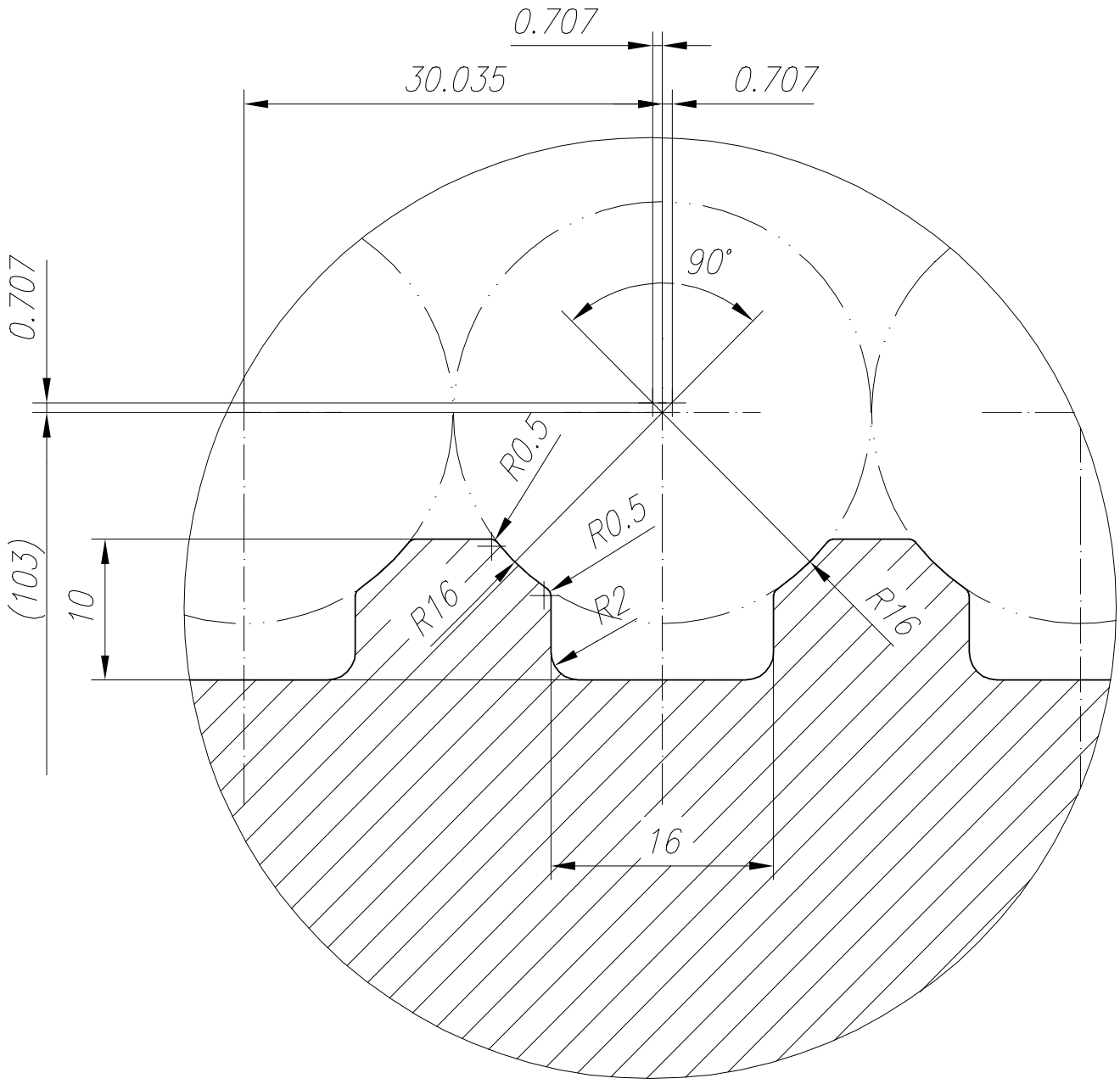

Figure 9: Design of the V-grooves of the comb modules.

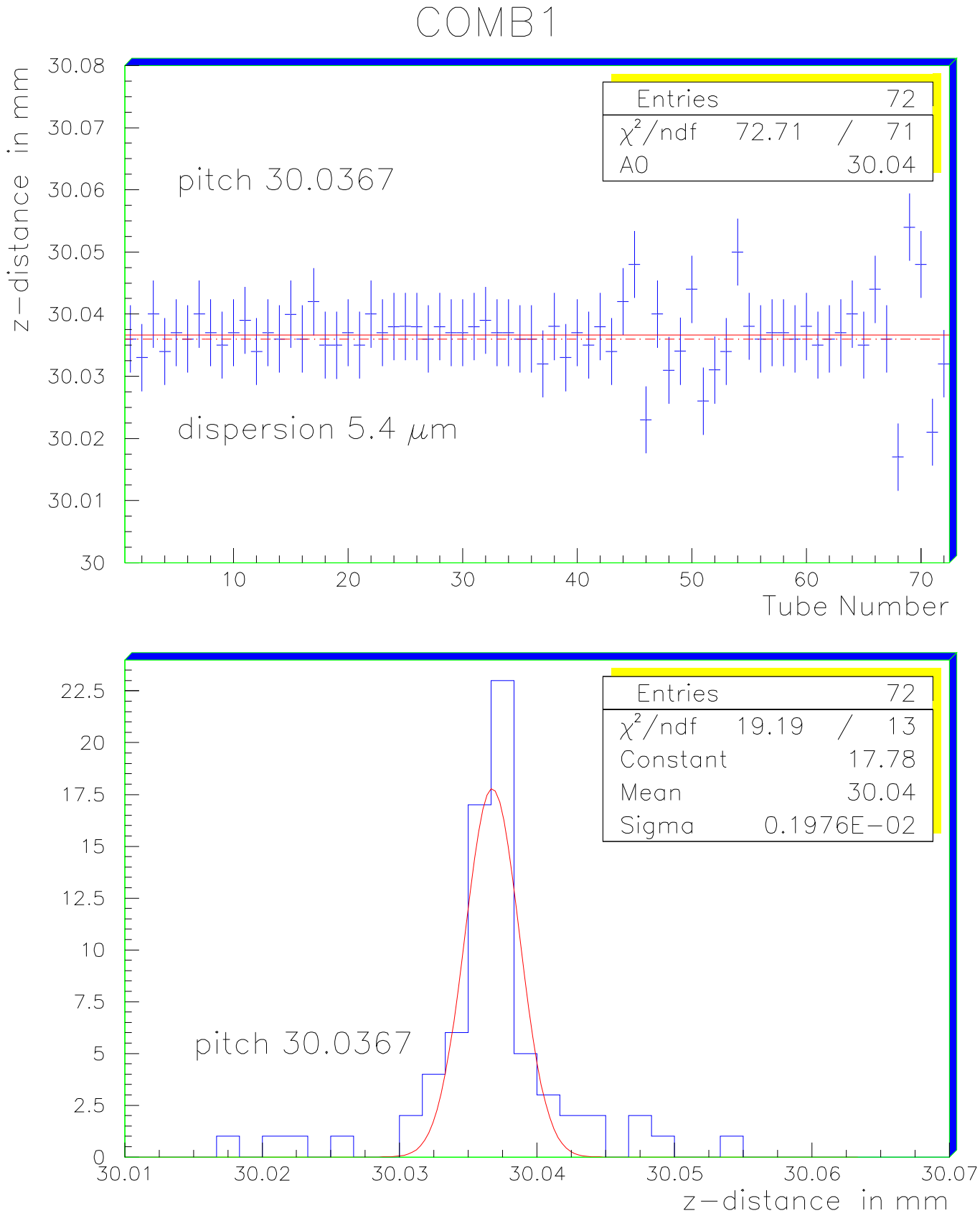

Figure 10: Measurement of the z-distances between the 72 V-grooves of one end comb line (comb no. 1) with precise steal cylinders of 30.000 mm diameter inserted in the grooves.

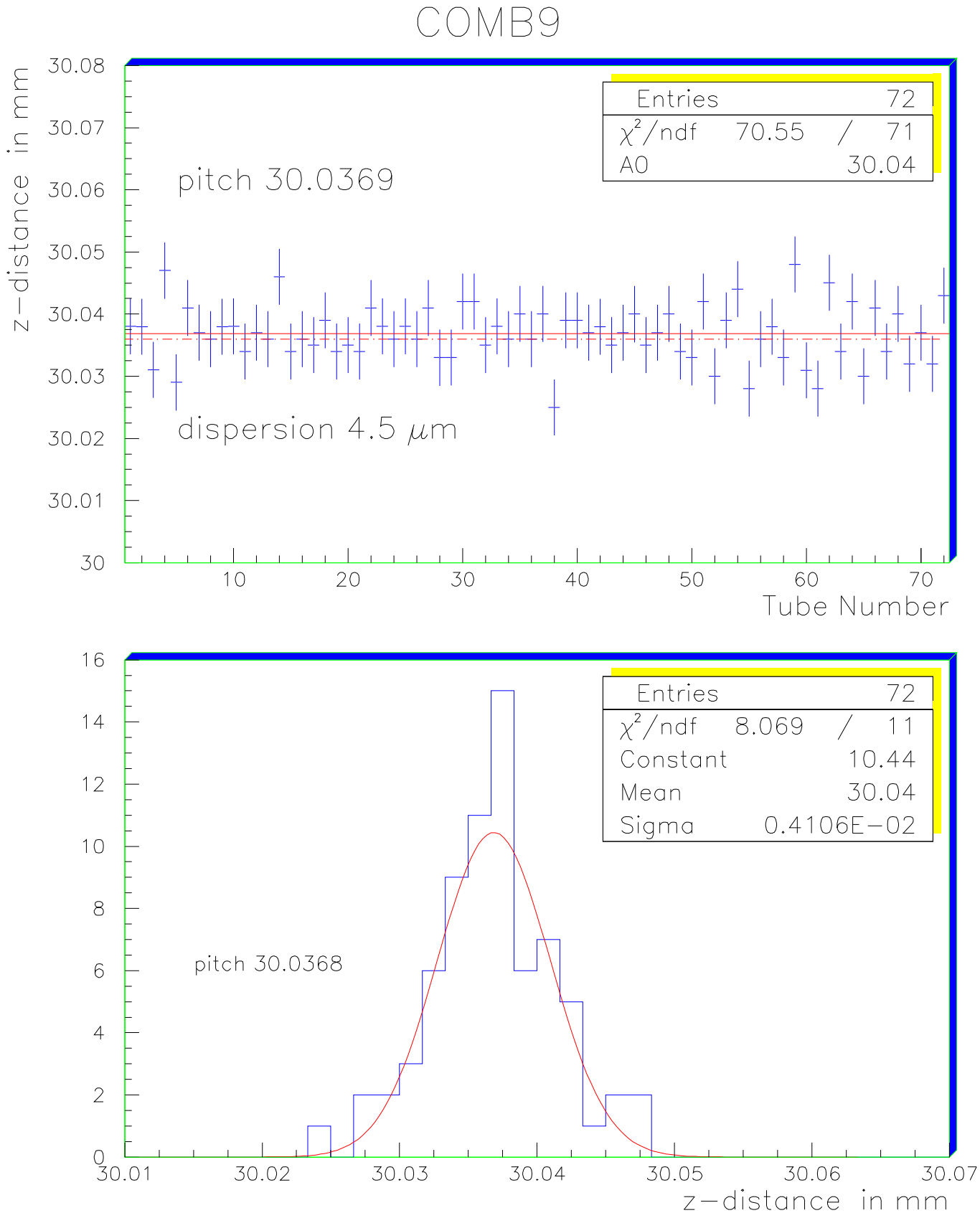

Figure 11: Measurement of the z-distances between the 72 V-grooves of the second end comb line (comb no. 9) with precise steal cylinders of 30.000 mm diameter inserted in the grooves.

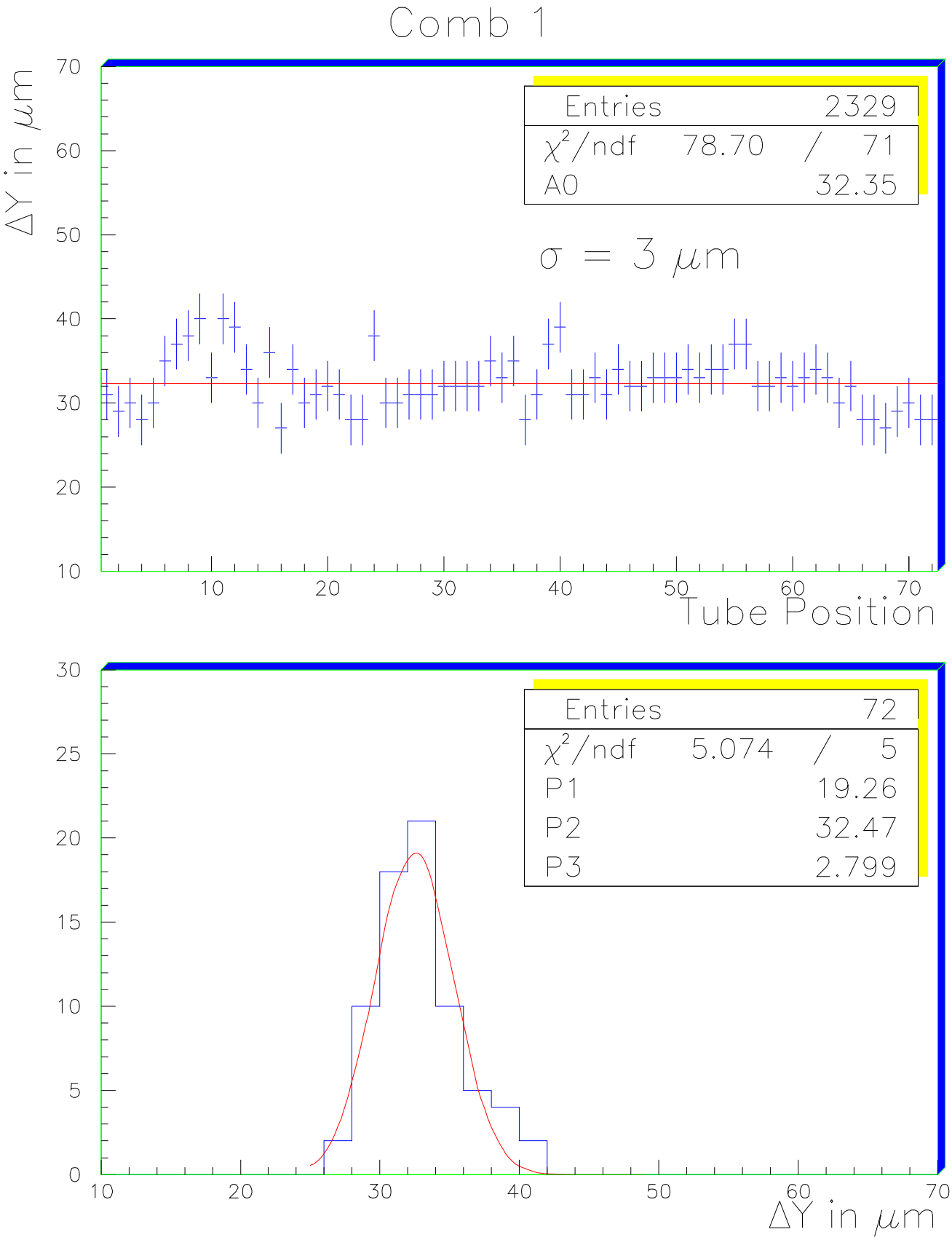

Figure 12: Measurement of the relative heights (y-coordinates) of the 72 V-grooves of one end comb line (comb no. 1) with a precise steal cylinder of 30.000 mm diameter inserted in the grooves. $\Delta y = 35$ μm corresponds to the nominal height to the top of the cylinder.

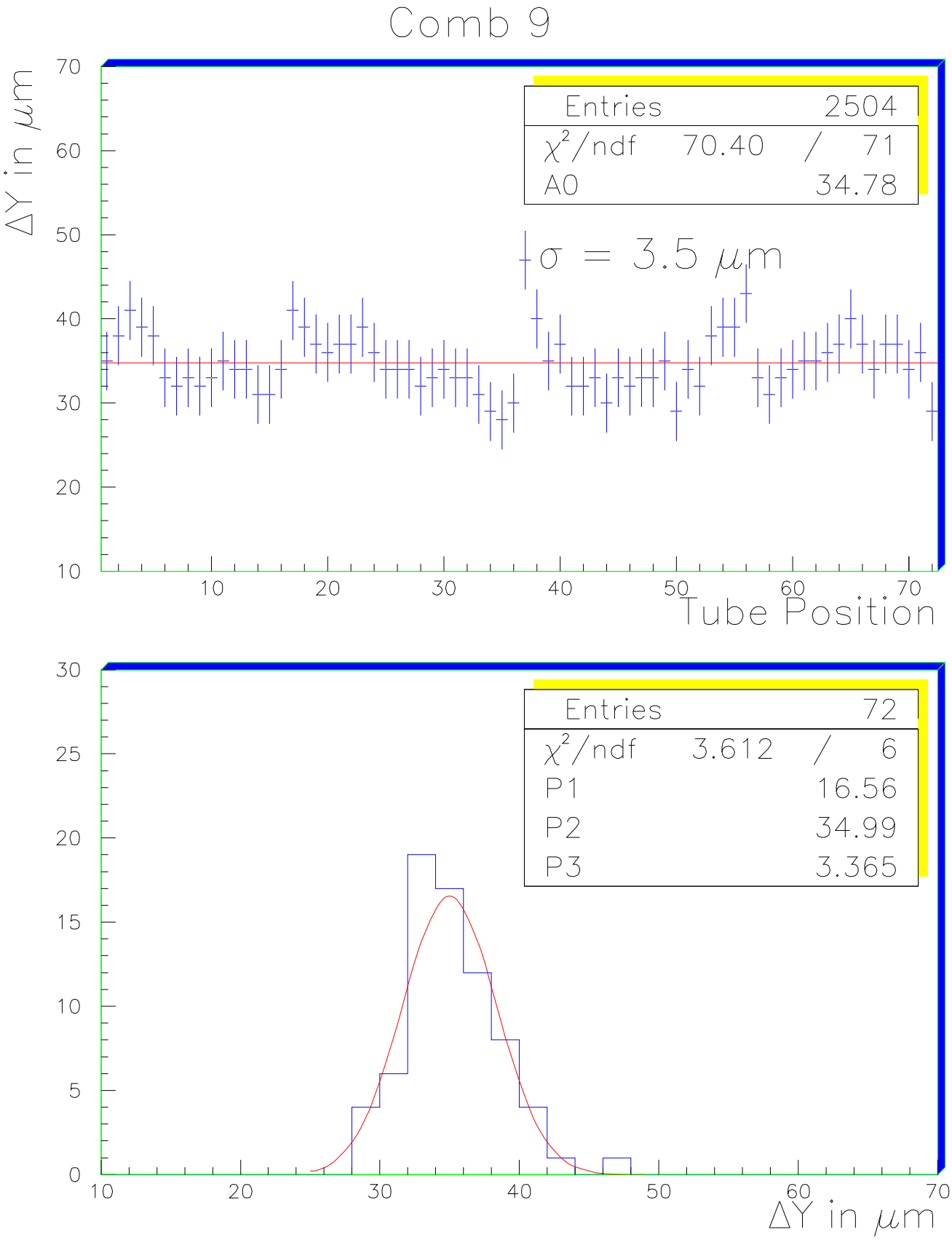

Figure 13: Measurement of the relative heights (y-coordinates) of the 72 V-grooves of the second end comb line (comb no. 9) with a precise steal cylinder of 30.000 mm diameter inserted in the grooves. $\Delta y = 35$ μm corresponds to the nominal height to the top of the cylinder.

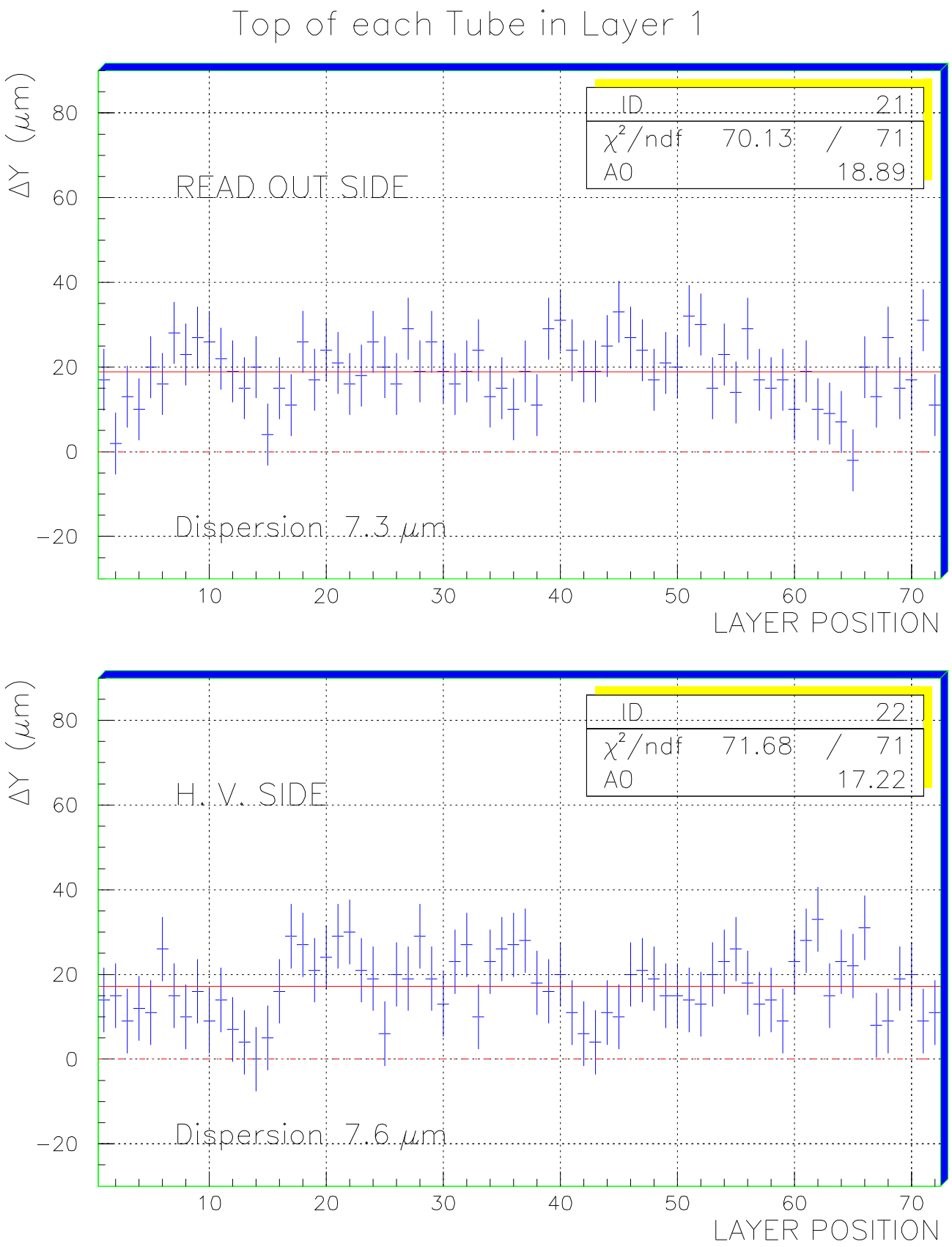

Figure 14: Measurement of the relative heights (y-coordinates) of 72 wired tubes in the two end combs on the HV side (comb no. 1) and on the readout side (comb no. 9). $\Delta y = 20$ μm corresponds to the height to the top of a tube of 29.985 mm outer diameter.

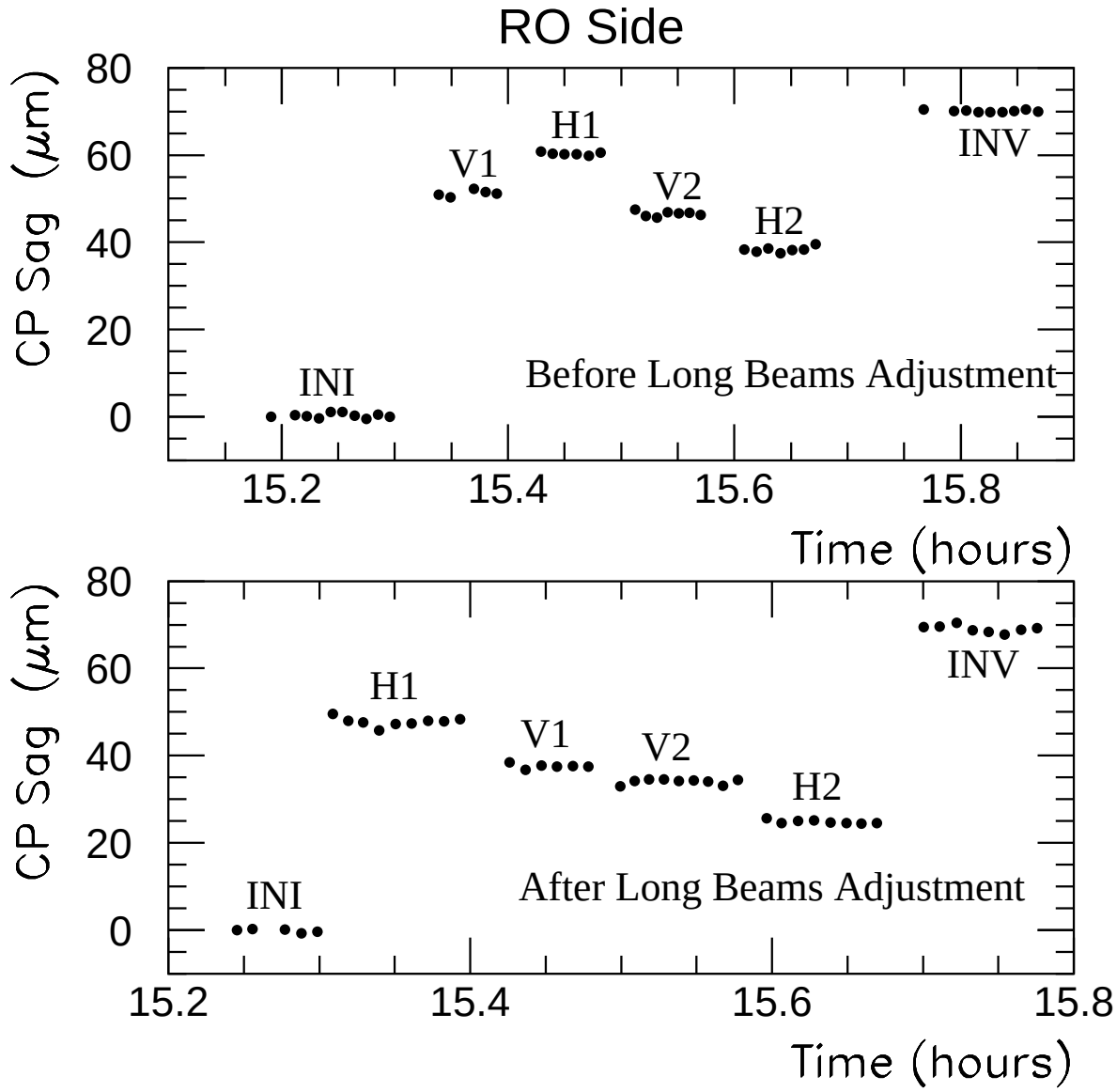

Figure 15: Readings of the RASNIK system on the readout (RO) side cross plate before and after long-beam adjustment (see text) for two positions of the spacer on the sphere supports, initial (INI) and inverted (INV) around the x axis, and for 4 positions of the spacer on the crane in the two vertical (V1, V2) and the two horizontal (H1, H2) orientations. After the long-beam adjustment the cross plate sag is symmetric for the initial and inverted with respect to the vertical (no sag) positions and can be determined as the average between the INI and INV readings.

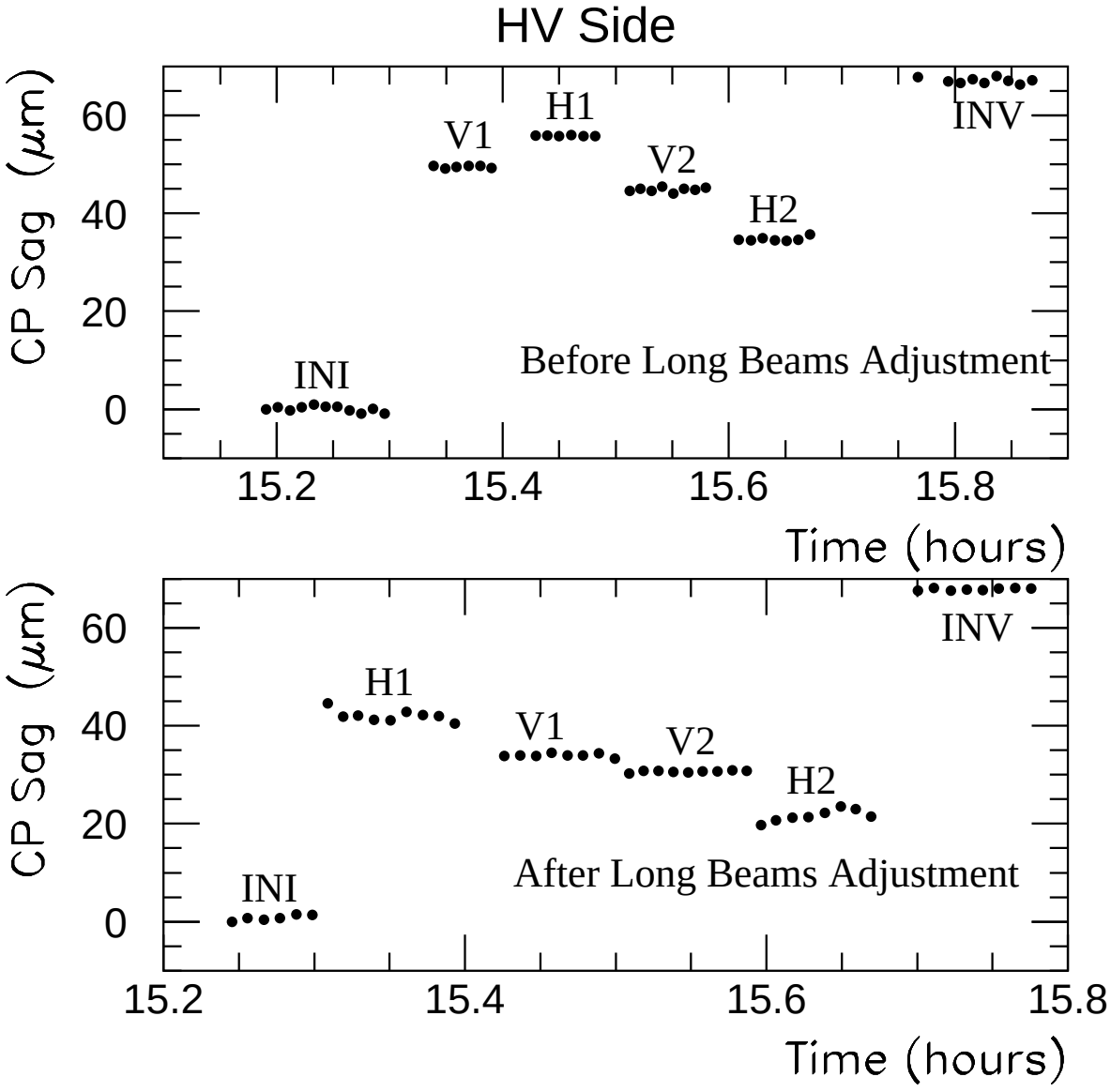

Figure 16: Same as Fig. 15 for the HV-side cross plate.

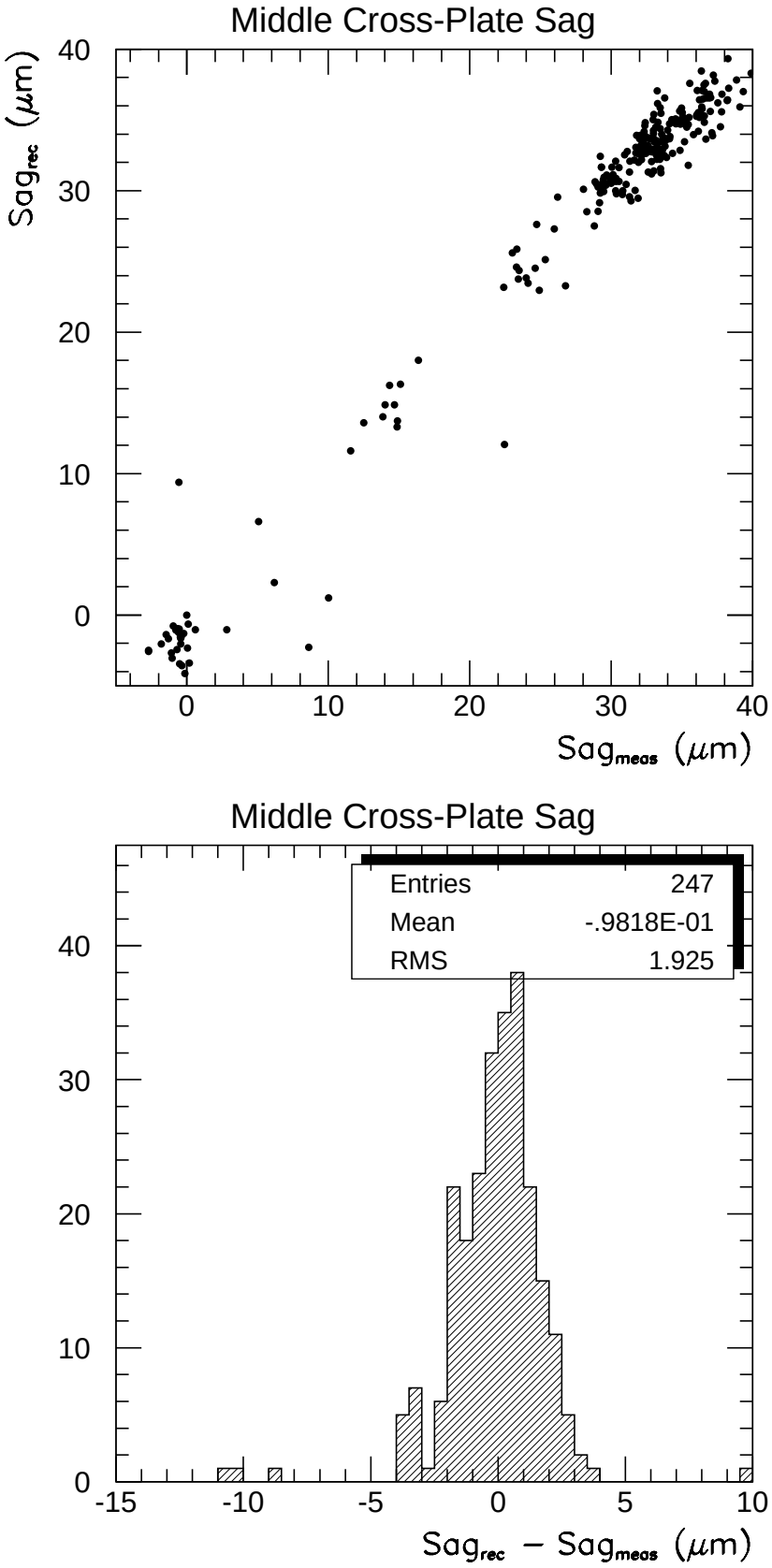

Figure 17: The sag of the middle cross plate measured with the on-cross-plate RASNIK system (Sag_{meas}) and reconstructed from the data of the in-plane alignment system and the on-cross-plate RASNIK systems on the outer cross plates (Sag_{rec}). Both determinations agree with high accuracy during all operations of the assembly of the first multilayer of the BOS chamber.

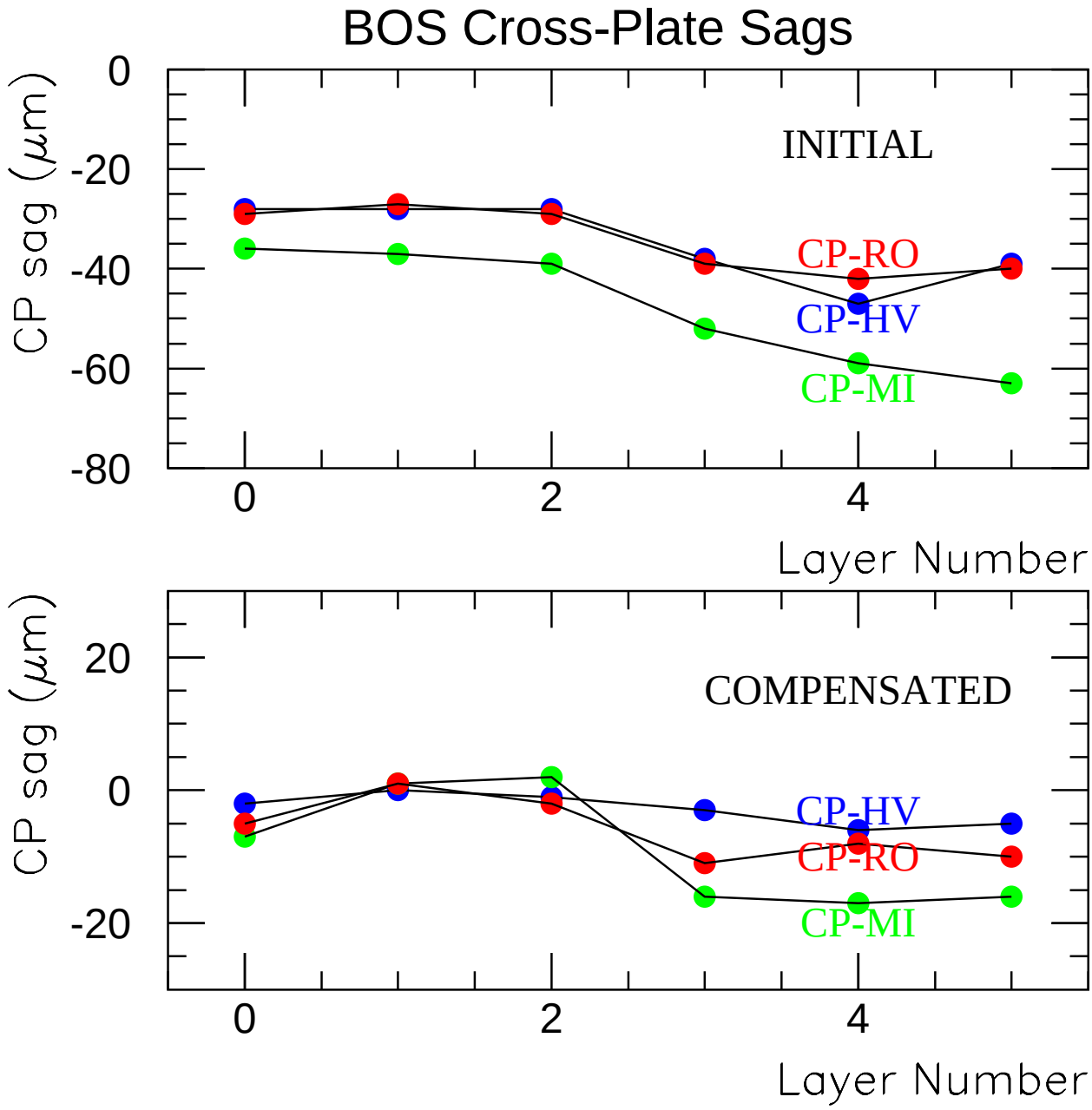

Figure 18: Sag of the three cross plates at the HV and readout (RO) ends and and in the middle of the chamber before and after sag compensation as measured with the on-cross plate RASNIK systems.

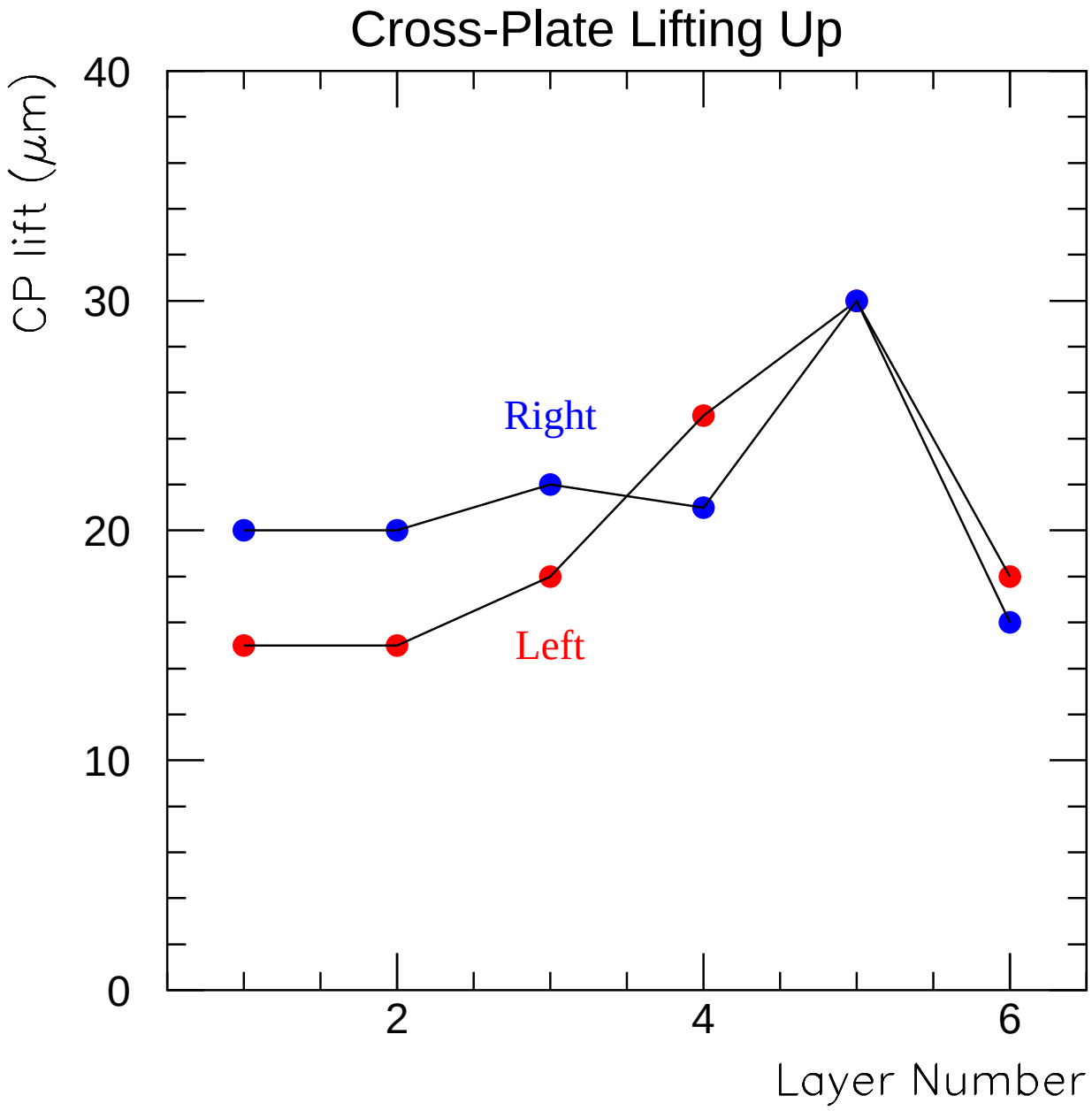

Figure 19: Lifting of the outer cross plates during force compensation with increasing number of tube layers glued as measured with the laser monitoring system with MPA-ALMY sensors.

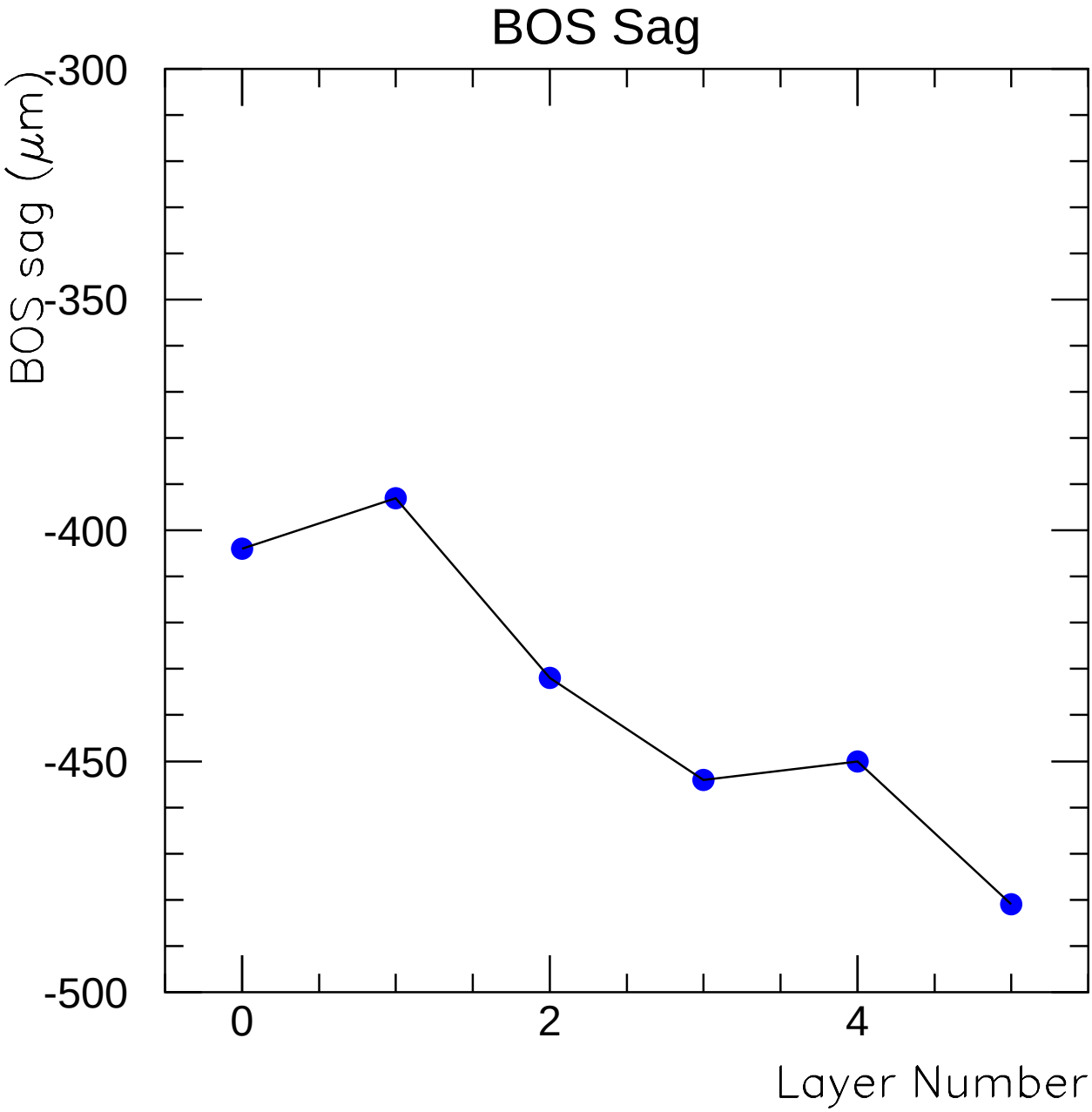

Figure 20: Average sag of the chamber along the x-direction with increasing number of tube layers glued measured with the two longitudinal RASNIK monitors (averaged).

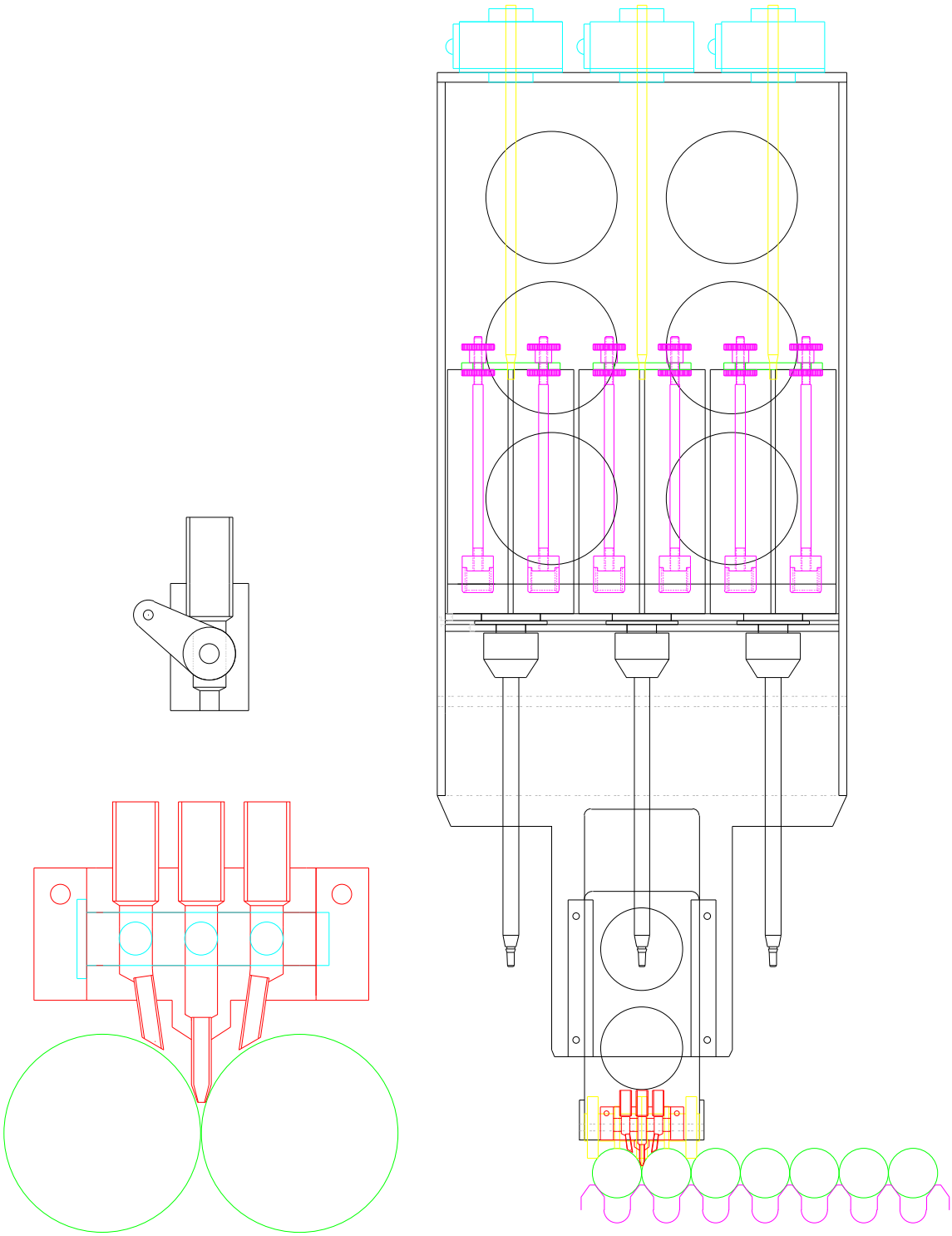

Figure 21: Components of a glue dispenser head. Each glue dispenser head produces three well defined glue ropes along the tubes. For each glue rope, the two-component glue is driven by a motor through the mixer and and the glue outlets with adjustable speed. Two of the glue dispensers are simultaneously moved along the tubes on rails (see Fig. 25). The glue distribution can be shut off at any x-position automatically, in particular at the tube ends.

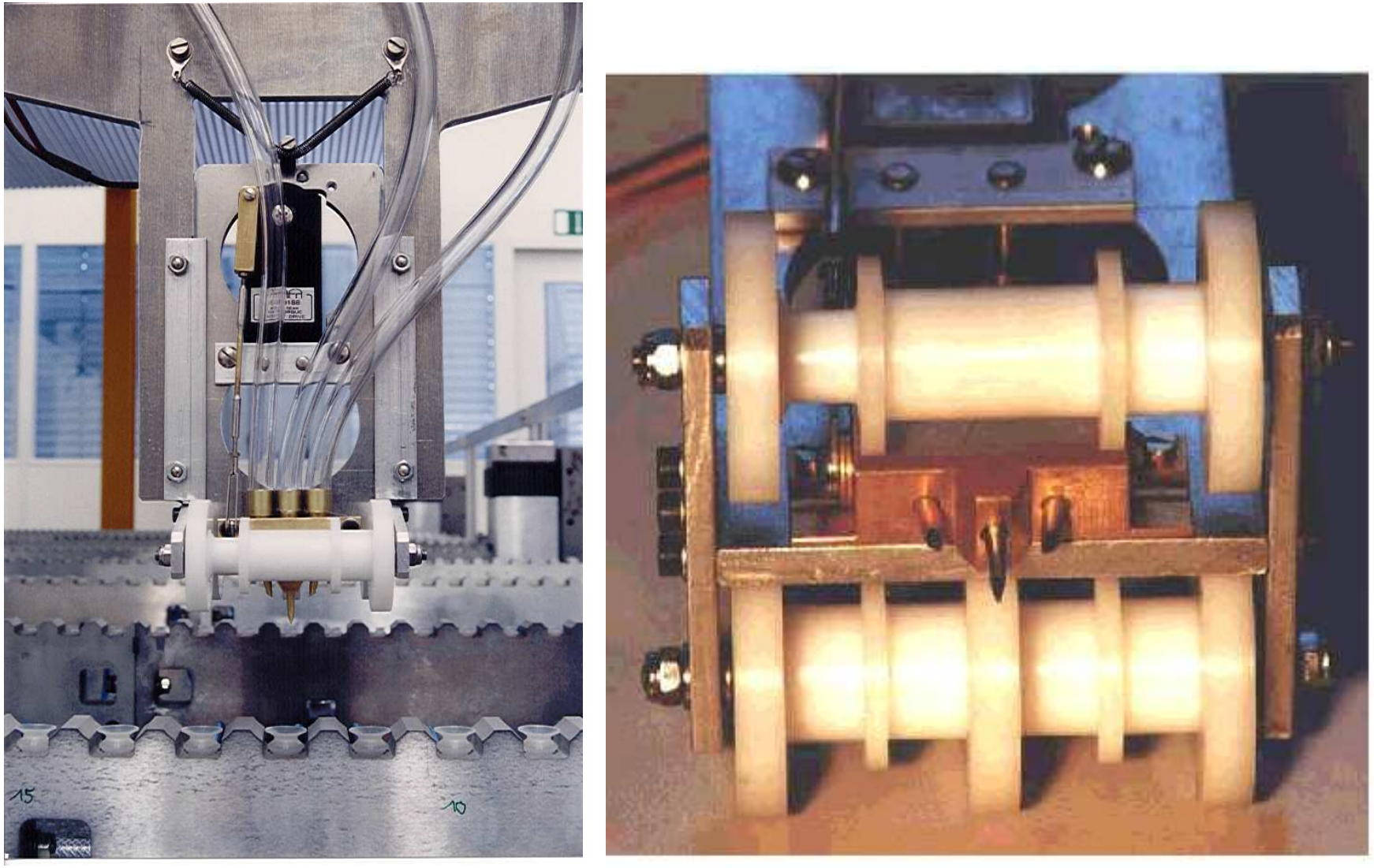

Figure 22: Pictures of the glue dispenser head used for the BOS prototype chamber.

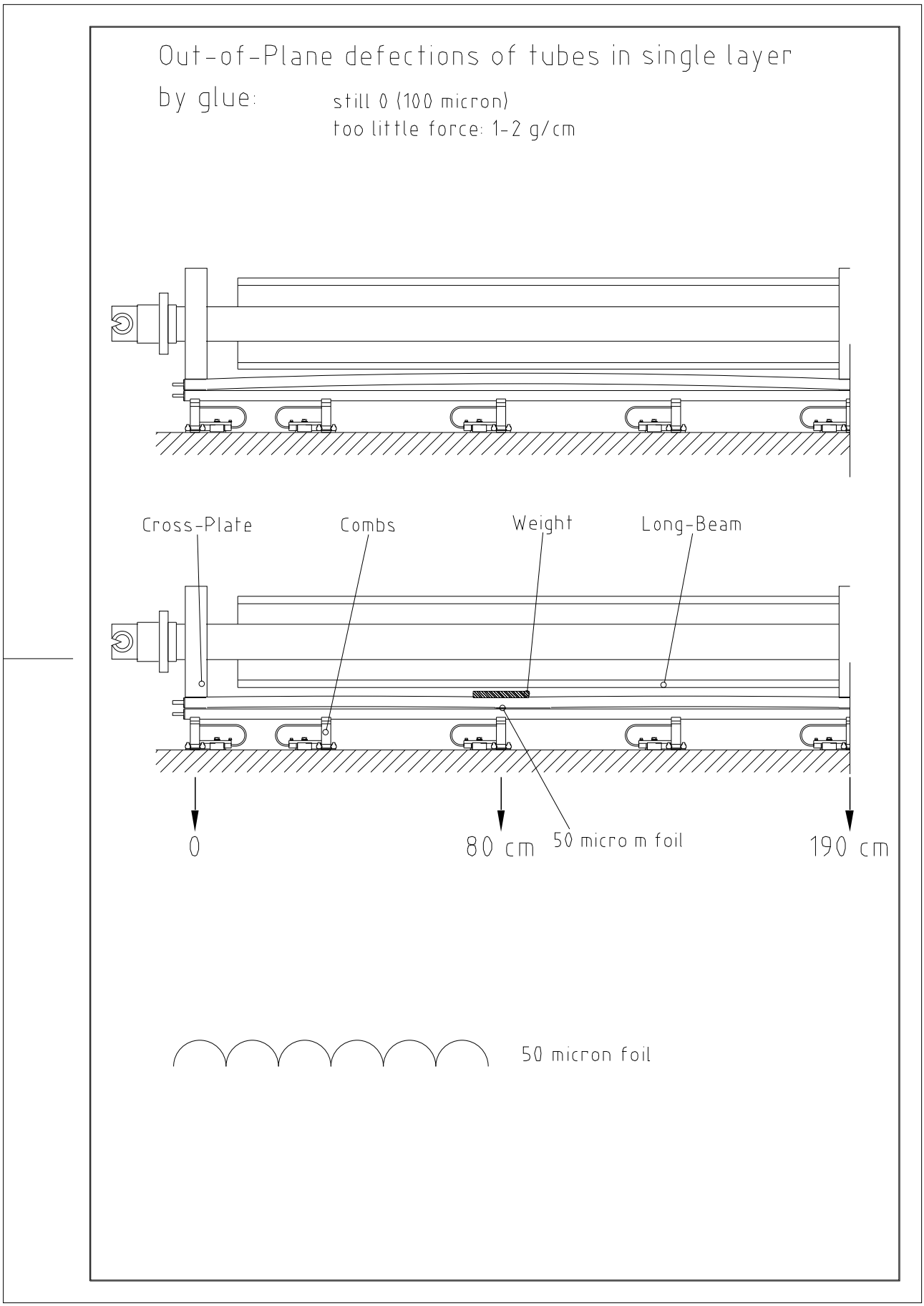

Figure 23: Illustration of out-of-plane deflections of tubes due to the glue and their control by using spacer foils and weights when two tube layers are glued together.

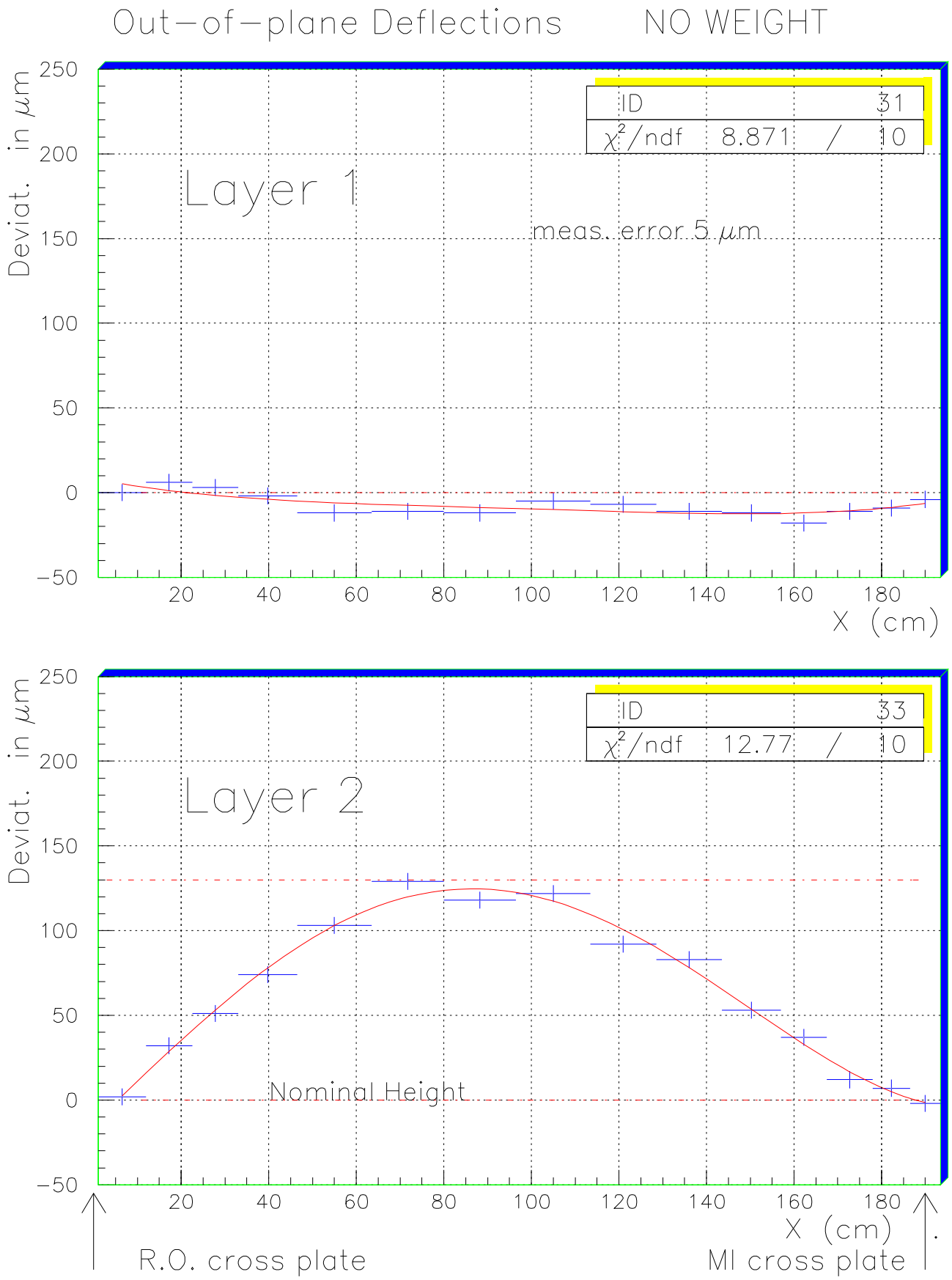

Figure 24: Out-of-plane deflection from the nominal tube height above the granite table in the top tube layer on the spacer caused by the glue between the tube layers in comparison with the measurement of the tube height along the tube in the bottom layer in the precision combs.

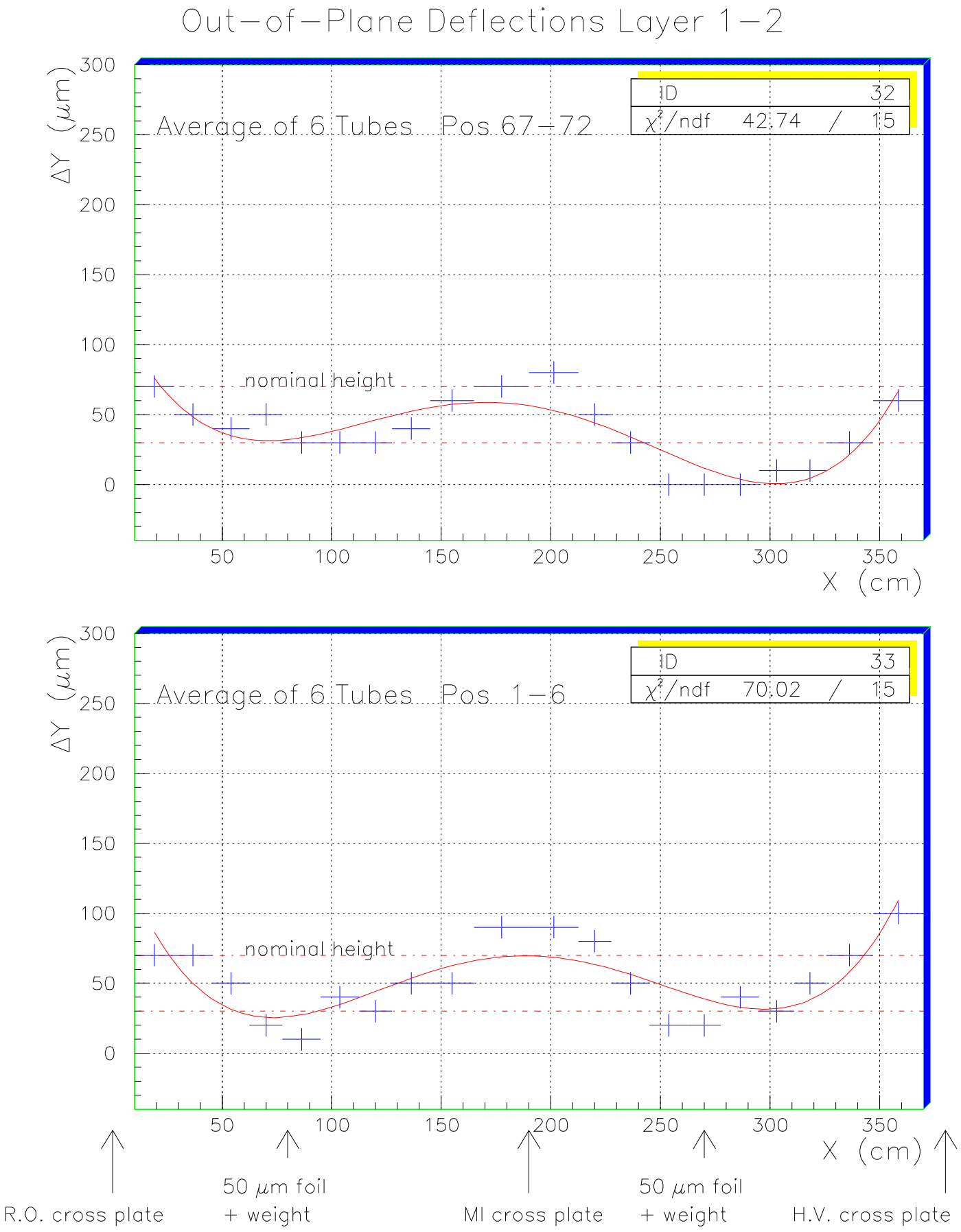

Figure 25: Out-of-plane deflections in layer 1 (of multilayer 1) suppressed by weights on top of the tube layer and using spacer foils between the layers during glueing of layer 2 (see text).

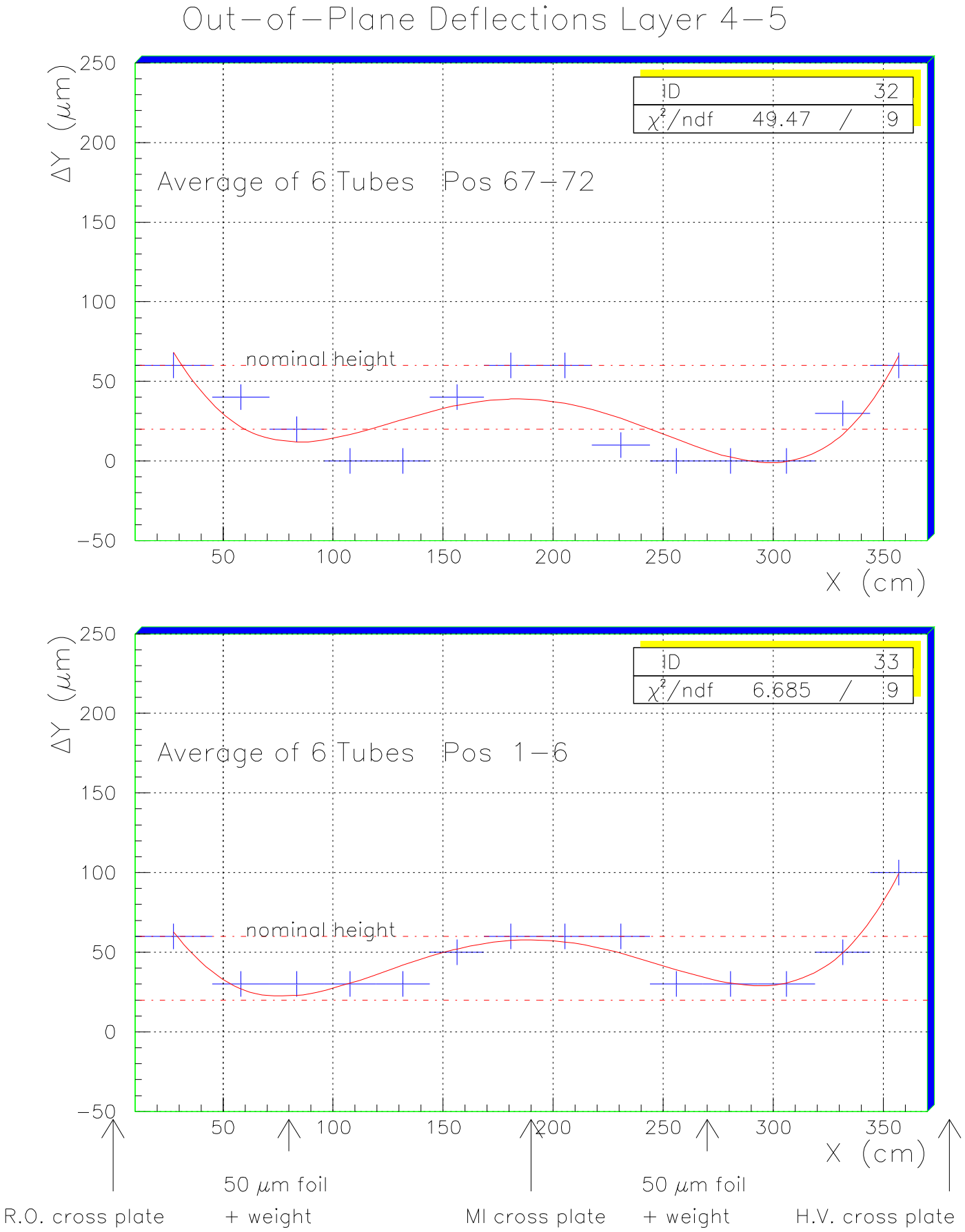

Figure 26: Out-of-plane deflections in layer 4 (of multilayer 2) suppressed by weights on top of the tube layer and using spacer foils between the layers during glueing of layer 5 (see text).

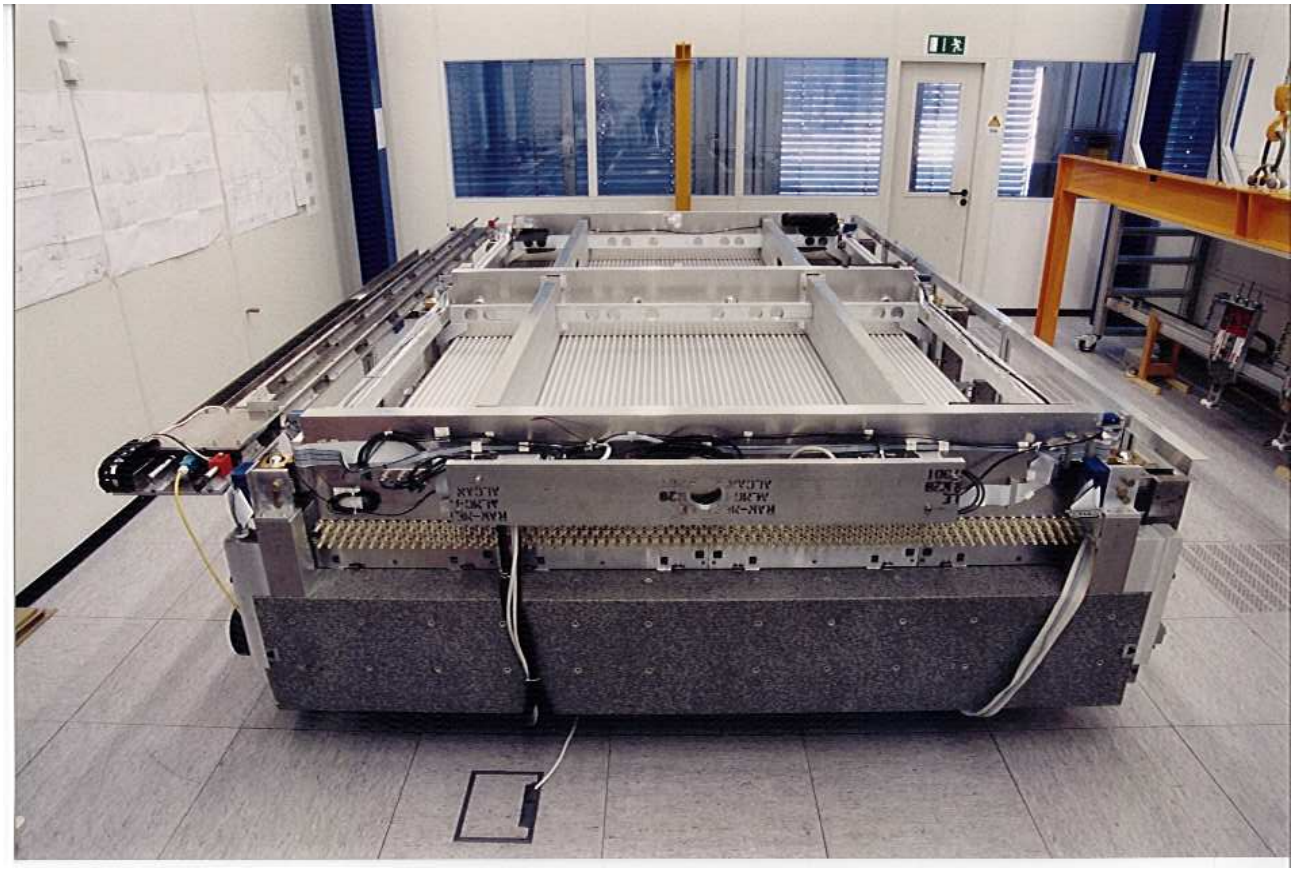

Figure 27: Glueing of the third layer in the first multilayer of the BOS prototype chamber.

Figure 28: The BOS prototype chamber during assembly with the first multilayer completed. The glue dispenser with its two moveable heads is installed for the next tube layer.

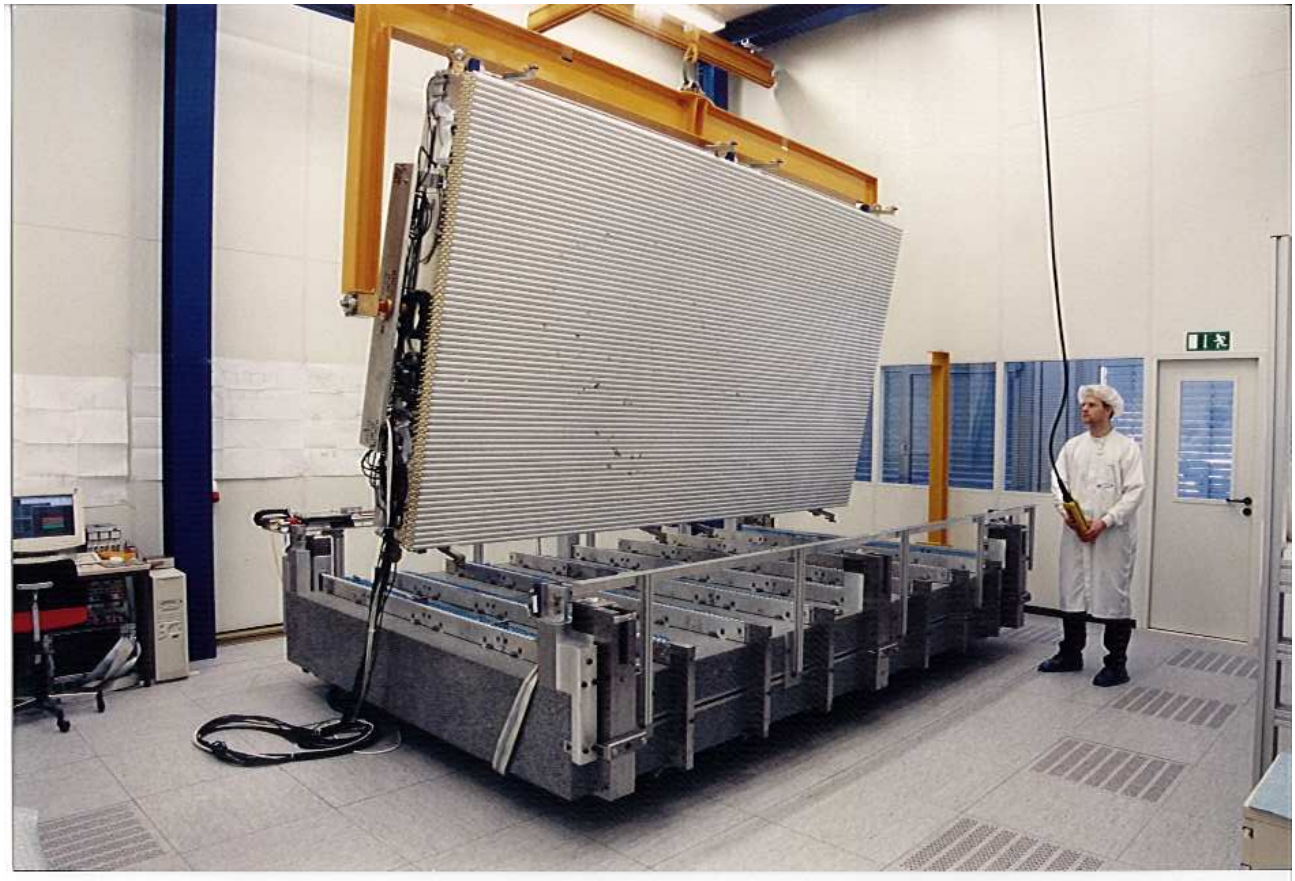

Figure 29: Rotation of the BOS chamber on the crane during assembly.

Figure 30: The BOS prototype chamber after completion set up in the test beam area at CERN.

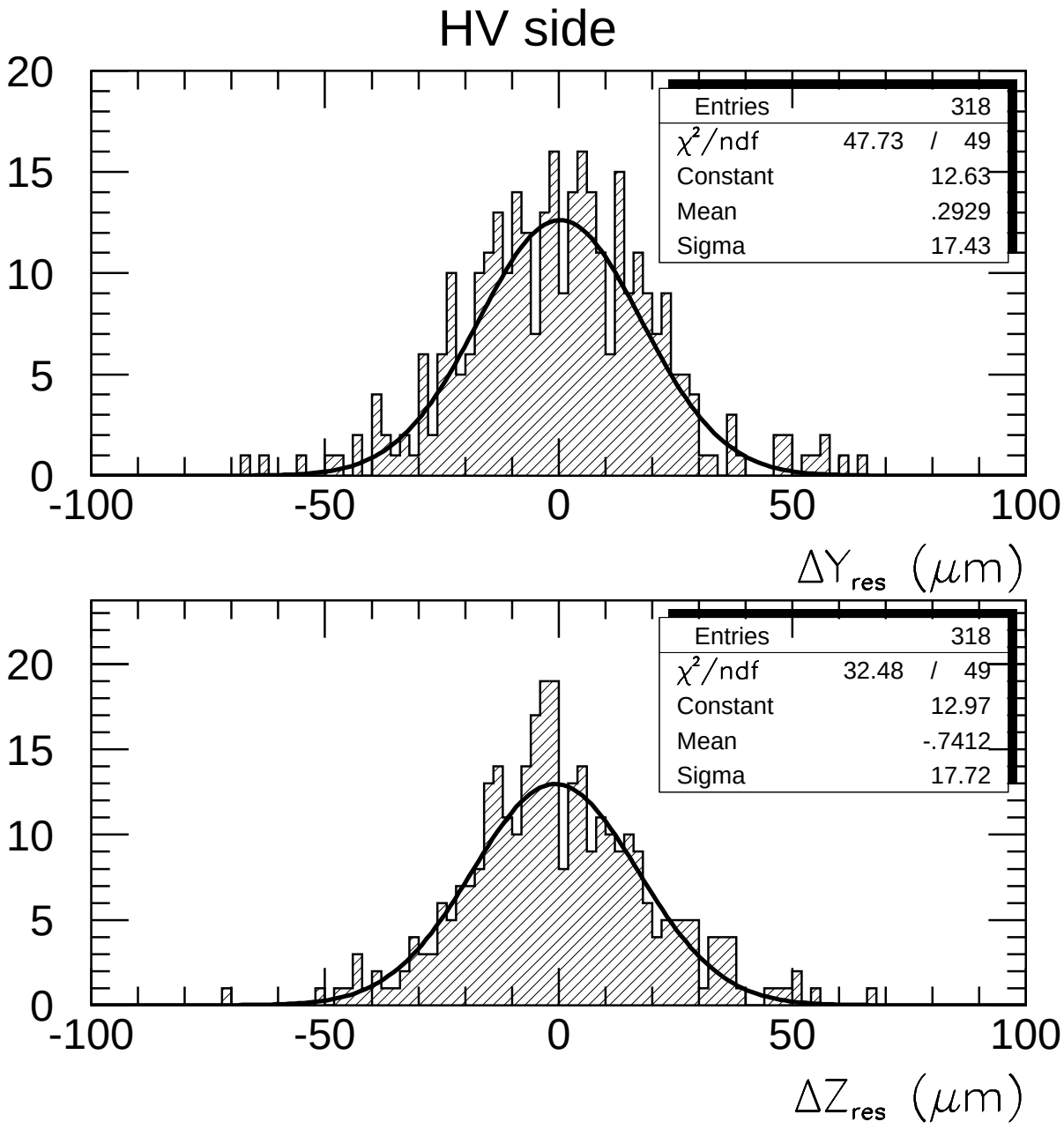

Figure 31: Distributions of the residuals of X-ray tomograph measured wire positions in y and z relative to a fixed grid (see text) for the scan on the HV side.

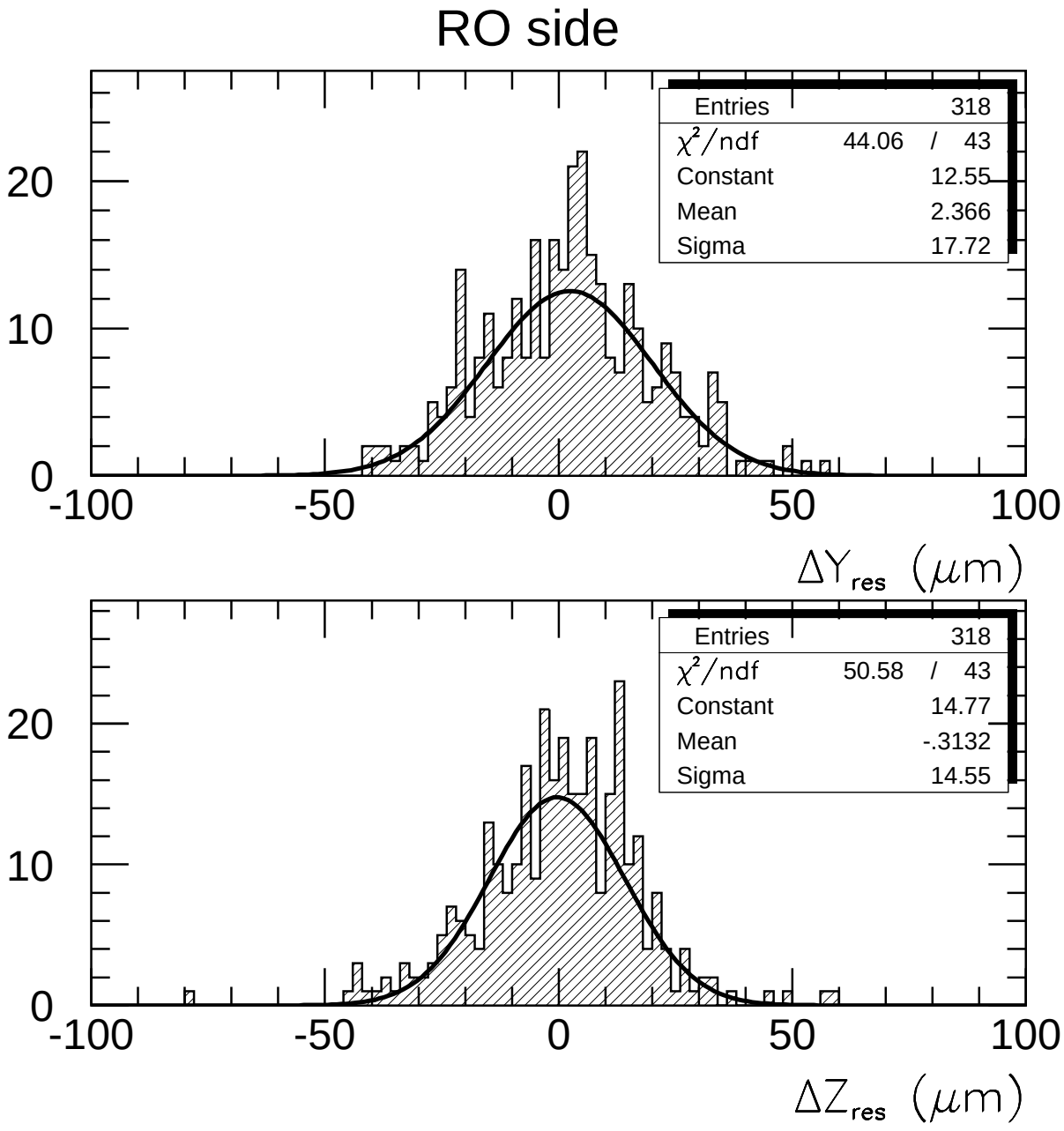

Figure 32: Distributions of the residuals of X-ray tomograph measured wire positions in y and z relative to a fixed grid (see text) for the scan on the readout side.

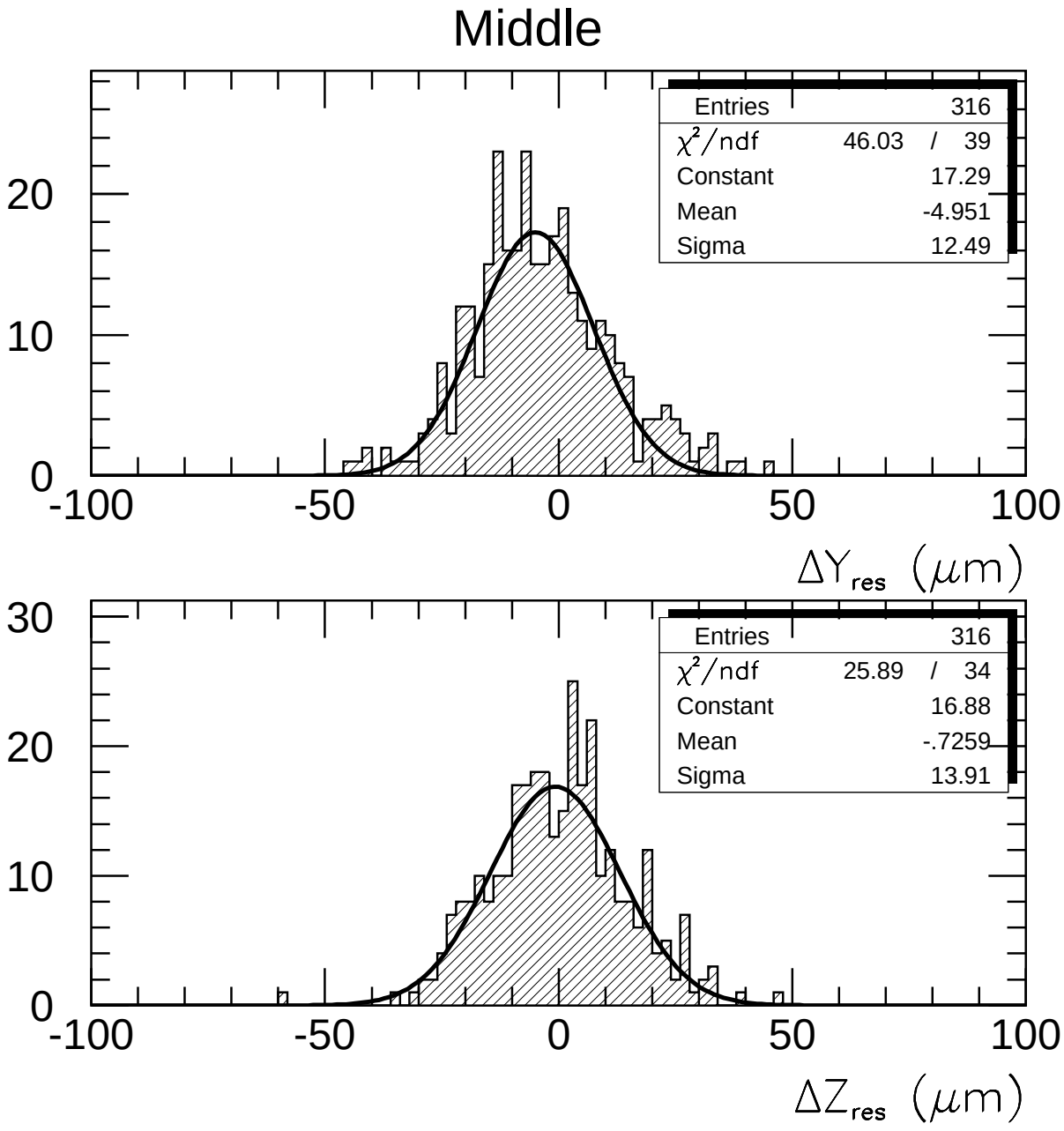

Figure 33: Distributions of the residuals of X-ray tomograph measured wire positions in y and z relative to a fixed grid (see text) for the scan along the middle cross plate.

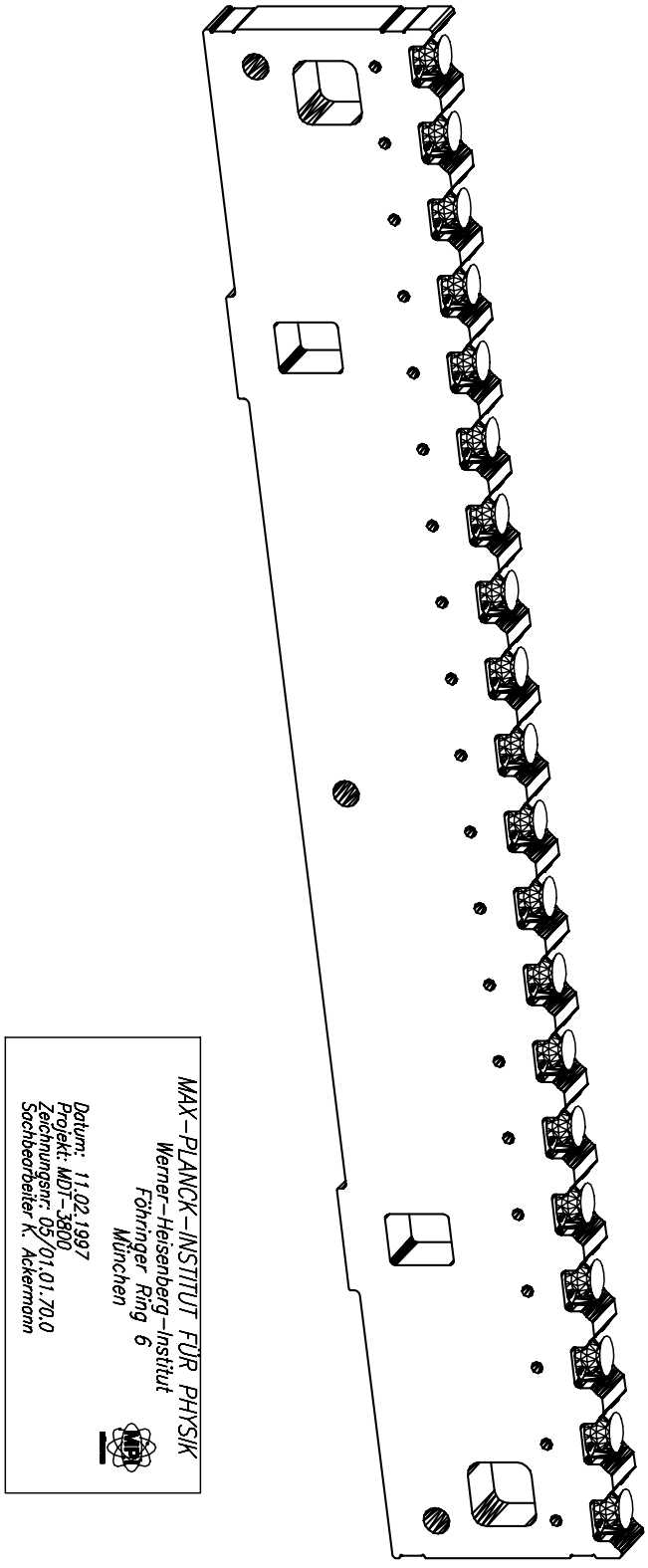

Figure A1: 3D drawing of a comb module.

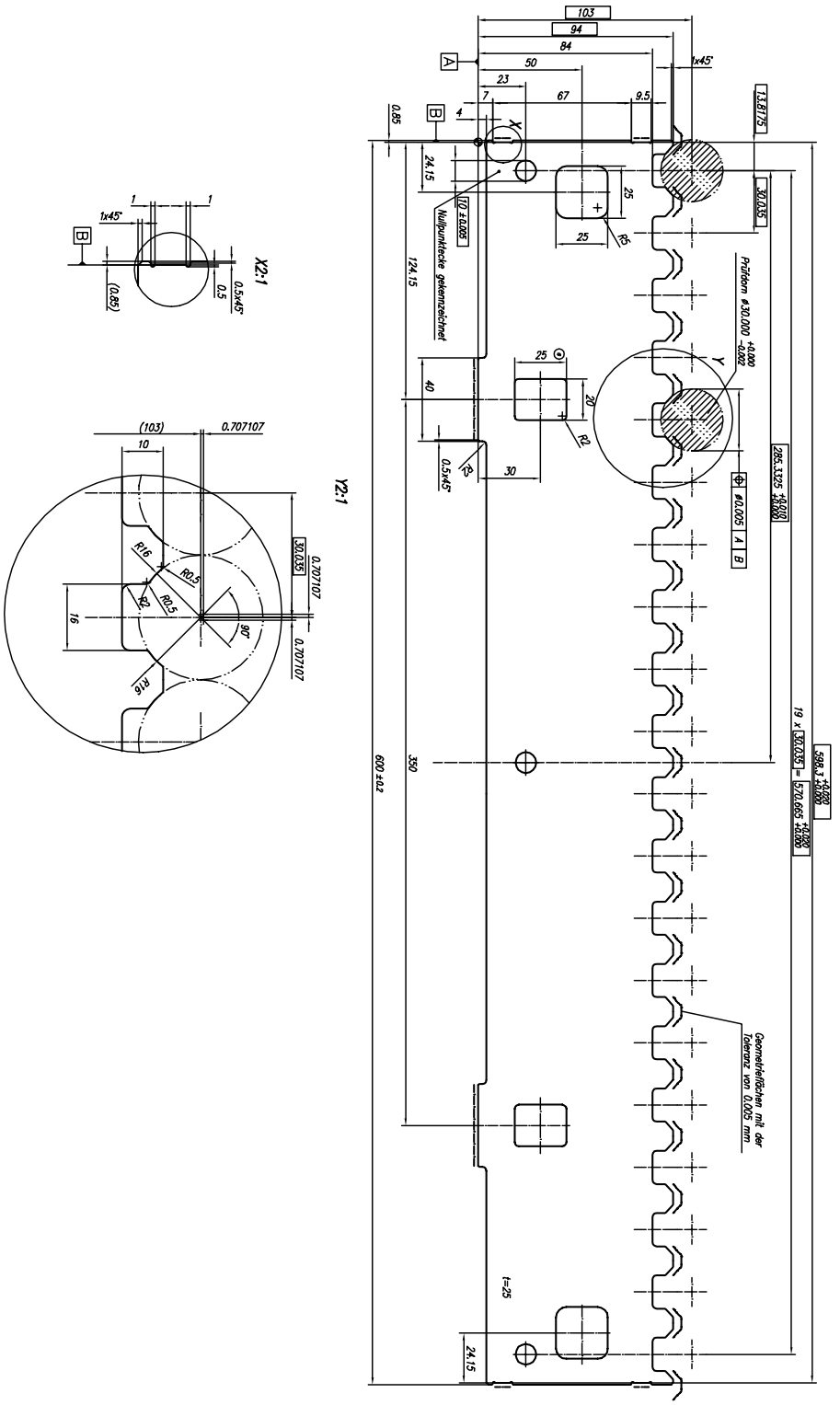

Figure A2: Production drawing for the wire erosion of a comb module.

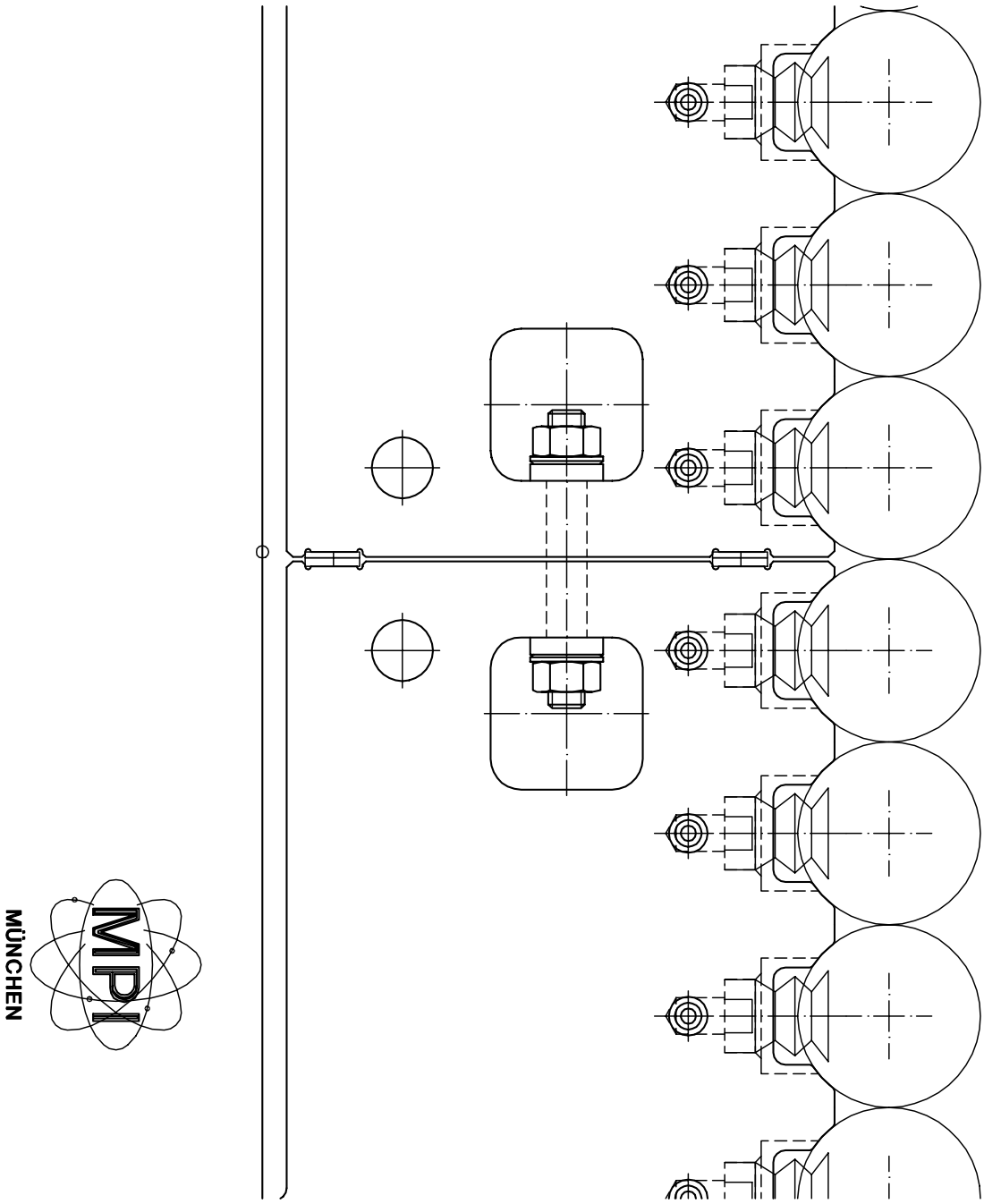

Figure A3: Interconnection between two adjacent comb modules.

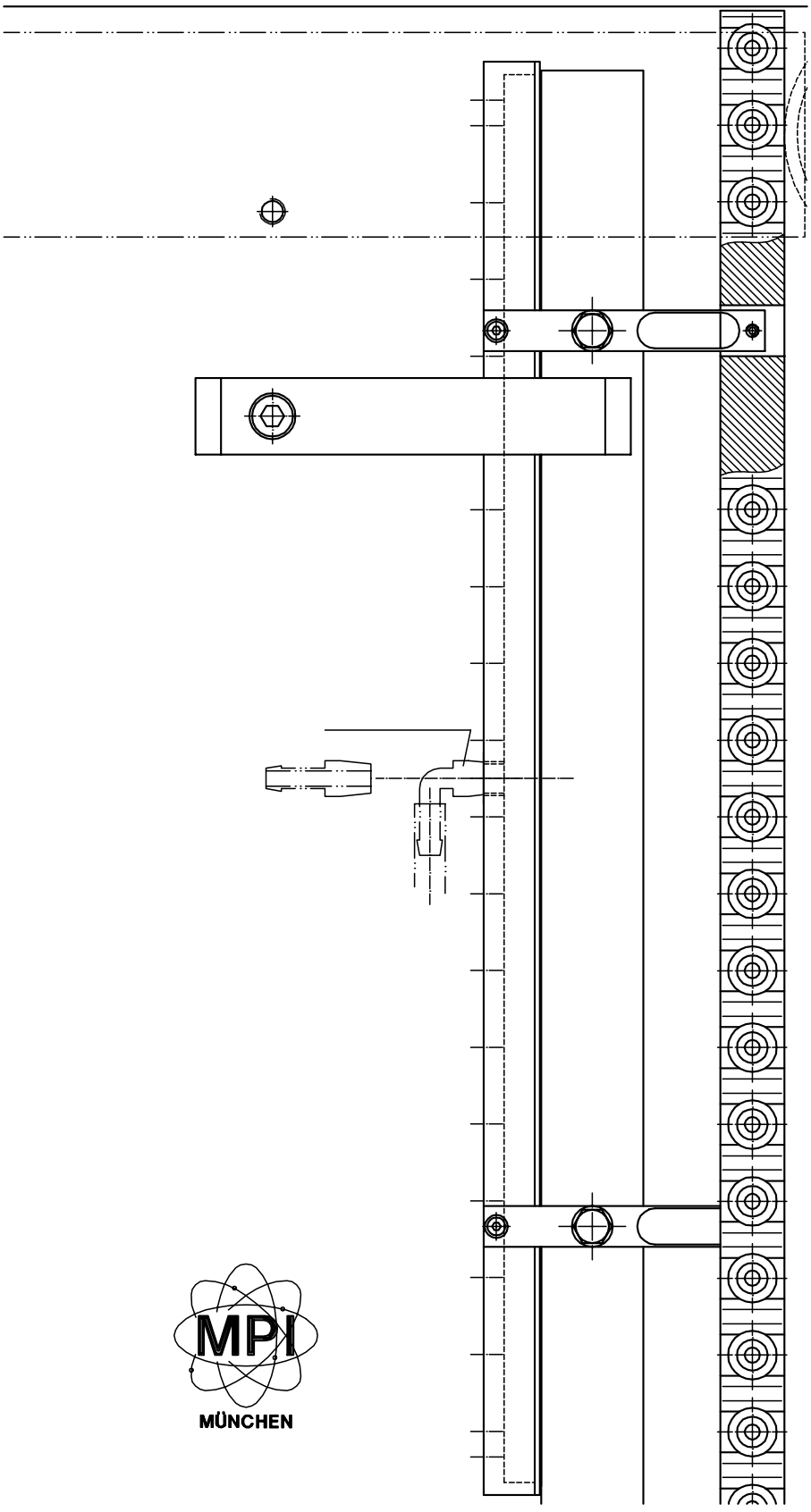

Figure A4: Top view of comb fixation and adjustment on the granite table.

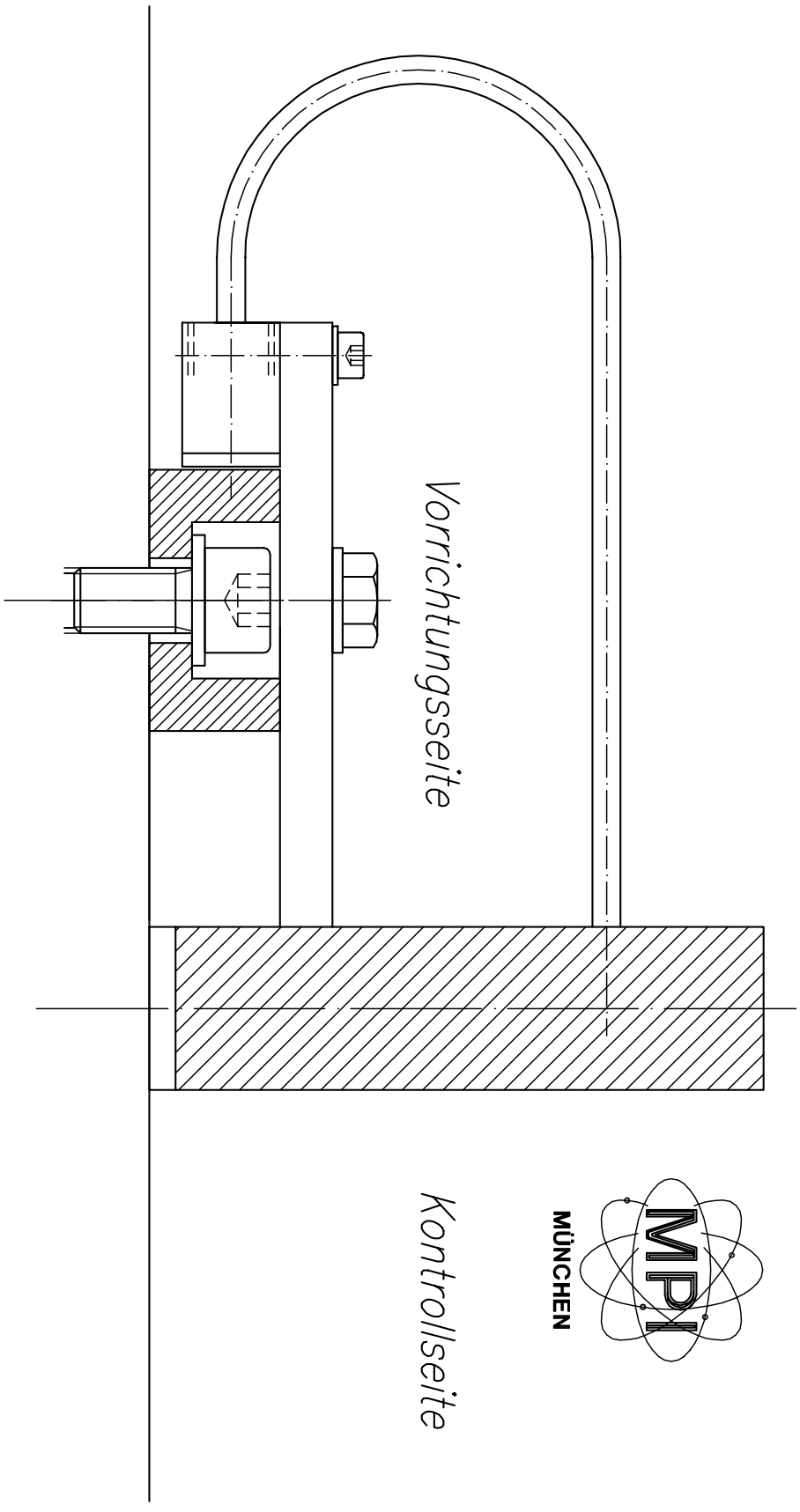

Figure A5: Fixation of combs on the granite table.

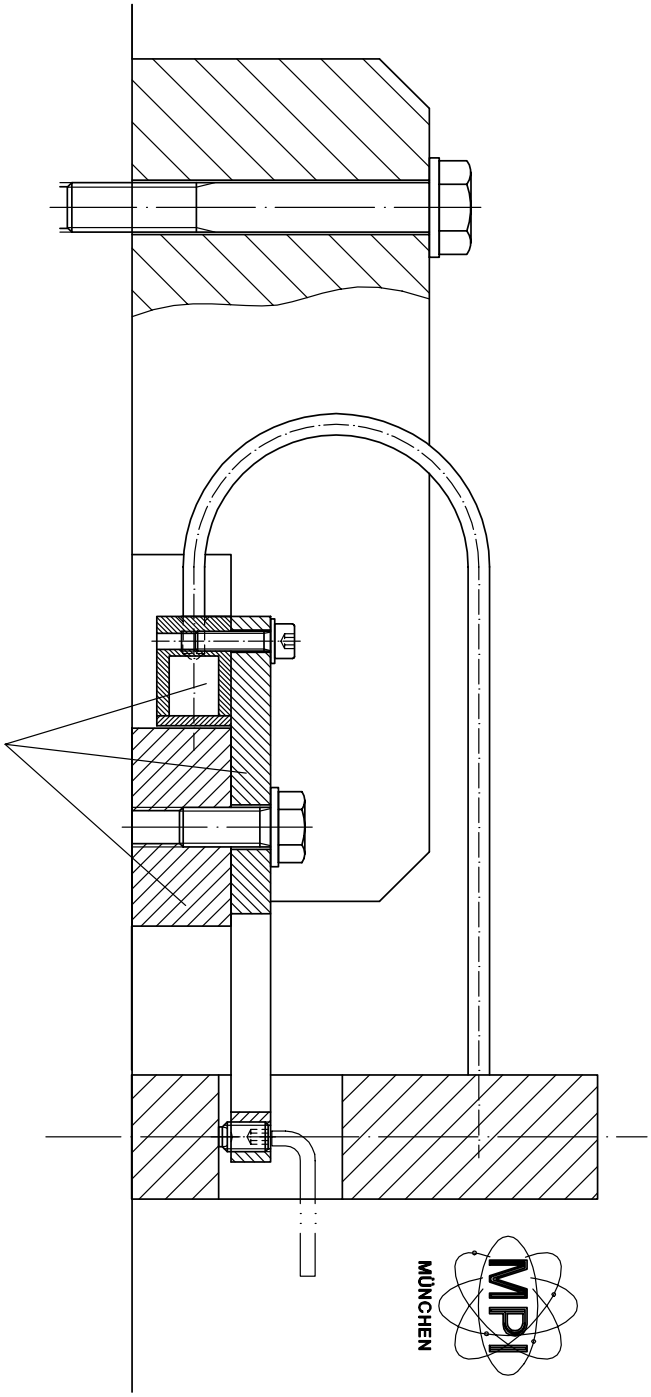

Figure A6: Fixation of combs to the granite table and vacuum distribution.

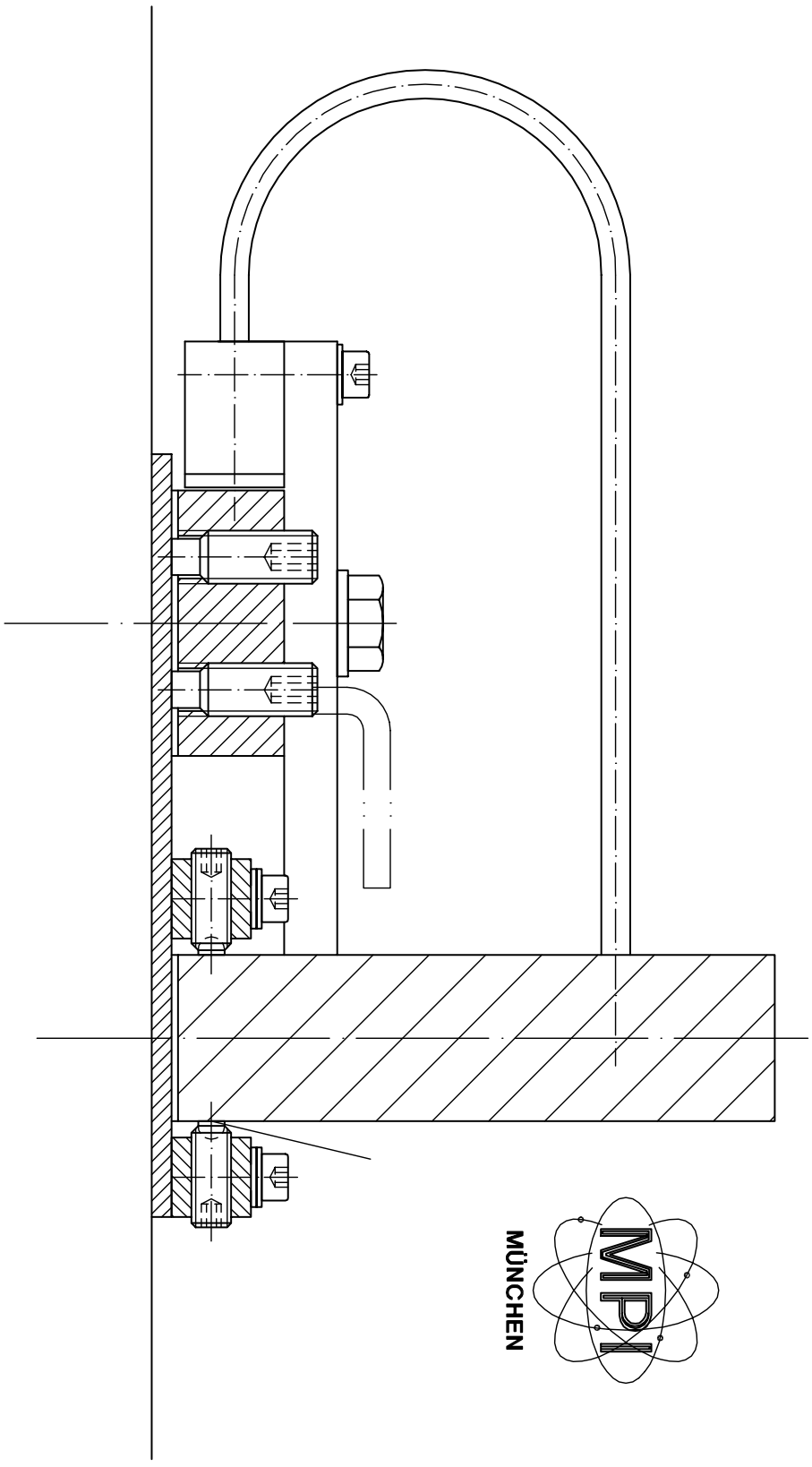

Figure A7: Adjustment of combs in x.

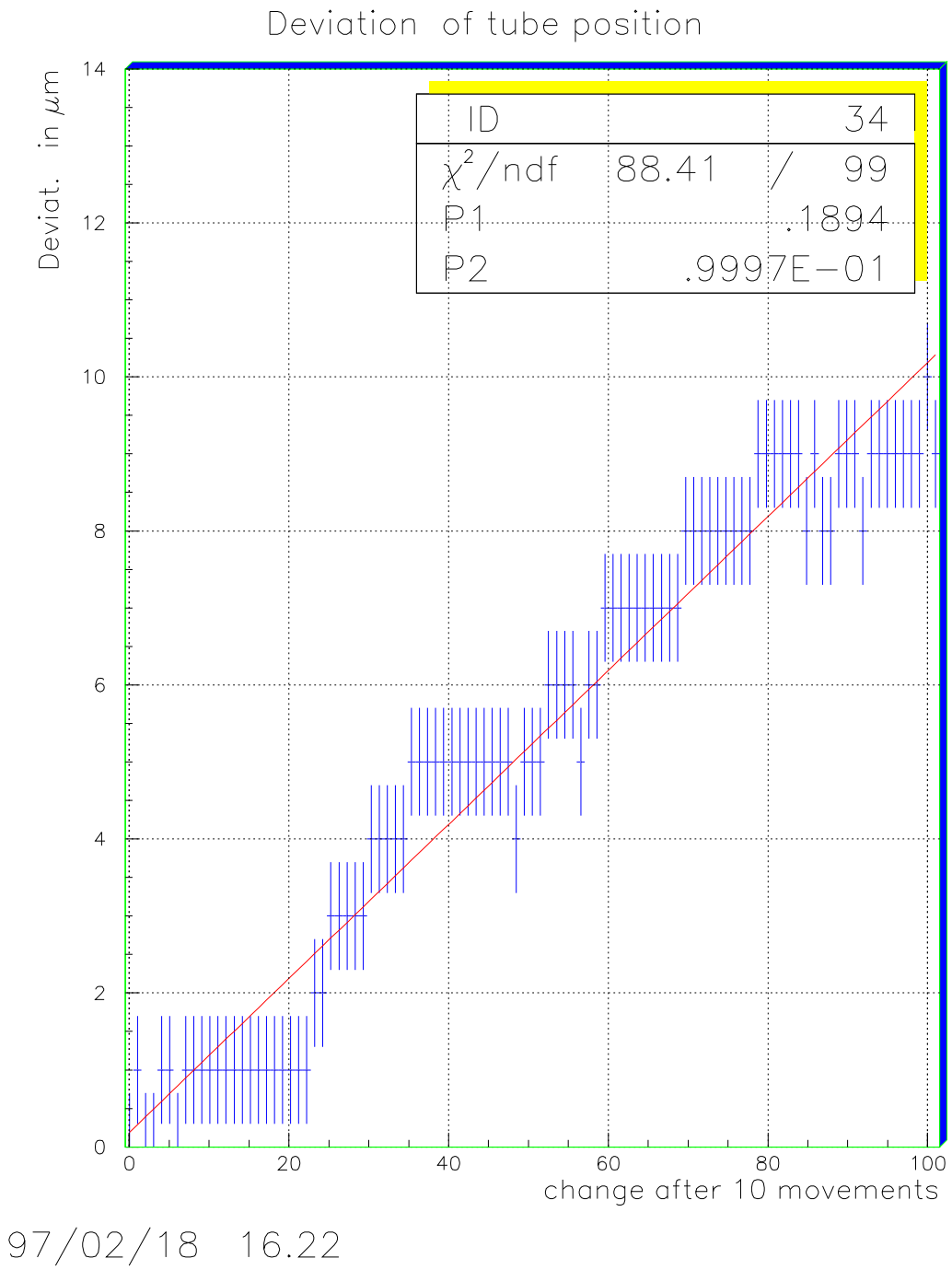

Figure A8: Change in y position over 1000 trials (100 measurements) of inserting a tube in a V-groove of a comb module.